

Higher fungal diversity is correlated with lower CO₂ emissions from dead wood in a natural forest: BioRxiv preprint

Chunyan Yang^{1,*}, Douglas A. Schaefer^{2,*}, Weijie Liu², Viorel D. Popescu³, Chenxue Yang¹, Xiaoyang Wang¹, Chunying Wu¹, Douglas W. Yu^{1,4,**}

¹ State Key Laboratory of Genetic Resources and Evolution, Kunming Institute of Zoology, Chinese Academy of Sciences, 32 Jiaochang East Rd., Kunming, Yunnan 650223 China

² Key Laboratory of Tropical Forest Ecology, Chinese Academy of Sciences, Xishuangbanna Tropical Botanical Garden, Menglun, Mengla, Yunnan 666303, China

³ Earth to Ocean Research Group, Department of Biological Sciences, Simon Fraser University, Burnaby, British Columbia V5A1S6, Canada

⁴ School of Biological Sciences, University of East Anglia, Norwich Research Park, Norwich, Norfolk NR47TJ UK

* These authors contributed equally.

** Corresponding author: tel: +4407510308272 and +8618608717369; fax: +441603592250; emails: dougwyu@gmail.com and douglas.yu@uea.ac.uk; Twitter: @insectsoup

Type of Paper: Primary Research Article

Abstract: 165 words

Main text: 4565 words

References: 63

Figures: 2

Tables: 2

Text boxes: 0

Abstract

Wood decomposition releases almost as much CO₂ to the atmosphere as does fossil-fuel combustion, so the factors regulating wood decomposition can affect global carbon cycling. We used metabarcoding to estimate the fungal species diversities of naturally colonized decomposing wood in subtropical China and, for the first time, compared them to concurrent measures of CO₂ emissions. Wood hosting more diverse fungal communities emitted less CO₂, with Shannon diversity explaining 26 to 44% of emissions variation. Community analysis supports a ‘pure diversity’ effect of fungi on decomposition rates and thus suggests that interference competition is an underlying mechanism. Our findings extend the results of published experiments using low-diversity, laboratory-inoculated wood to a high-diversity, natural system. We hypothesize that high levels of saprotrophic fungal biodiversity could be providing globally important ecosystem services by maintaining dead-wood habitats and by slowing the atmospheric contribution of CO₂ from the world’s stock of decomposing wood. However, large-scale surveys and controlled experimental tests in natural settings will be needed to test this hypothesis.

Introduction

Global decomposition of wood releases CO₂ (6 to 9.5 Pg C/year^{1, 2, 3}) at similar rates to fossil-fuel combustion (9.5 Pg C/year in 2011⁴). Decomposing wood also serves as essential habitat^{5, 6}. The factors controlling wood decomposition rates are therefore of broad importance to conservation and to carbon cycle-climate feedbacks.

However, temperature and moisture variables only explain minority portions of total variance in decomposition rates^{7, 8}. For instance, Bradford *et al.*⁹ reported that regional temperatures explain only 28% of local variance in mass loss.

The diversity of wood-decomposing fungi might explain much of the remaining unexplained variance. In laboratory-inoculation experiments using small numbers of culturable fungal species, wood pieces with higher final fungal diversity exhibited reduced decay rates^{10, 11, 12}. Inoculated wood placed in the field also showed a negative effect of final fungal species diversity on decay ($R^2 = 0.15^{13}$).

However, in contrast to laboratory experiments, natural wood decomposition involves much higher species diversity, more complex assembly histories, and selective faunal feeding on decomposers^{14, 15, 16}. Thus, it is important to examine the relationship between fungal diversity and decomposition rates in wood that is colonized and decomposing under natural conditions.

Natural fungal communities can be characterized using metabarcoding¹⁷, in which nuclear ribosomal internal transcribed spacer (ITS) regions are PCR-amplified and read using high-throughput sequencing^{18, 19, 20, 21}. ITS1 and ITS2 are each sufficiently variable to differentiate fungal species^{18, 19} and return similar estimates of OTU (Operational Taxonomic Units) richness and community structure^{19, 22}.

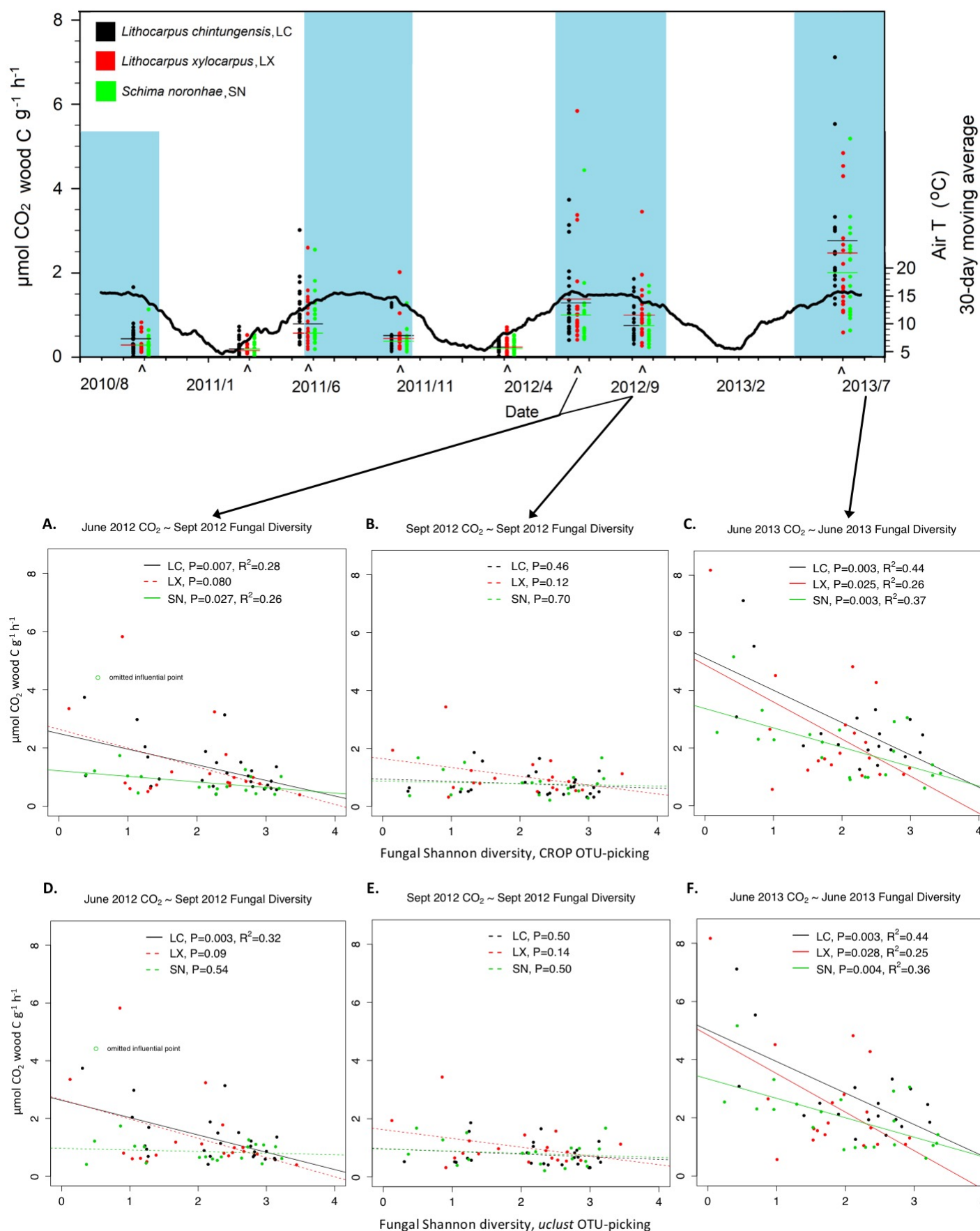
Here we metabarcoded ITS2 to examine fungal communities in naturally colonized wood pieces sampled across a wide range of decay classes in the Ailao Mountain forest of Yunnan, China. These wood pieces were sampled from a larger experiment involving three tree species (LC: *Lithocarpus chintungensis* [Fagaceae], LX: *L. xylocarpus*, and SN: *Schima noronhae* [Theaceae]) from which naturally occurring dead-wood pieces were regularly measured for CO₂ emission rates over three years⁸. We measured the extent to which variation in the species diversity and composition of fungal communities can explain variation in emission rates.

Results

Taxonomy results – Numbers of fungal OTUs ranged from 17 to 199 across wood pieces, tree species, and sampling dates, with means of 73.8 (LC, Sep 2012), 76.7 (LC, June 2013), 87.0 (LX, Sep 2012), 90.5 (LX, June 2013), 83.7 (SN, Sep 2012), and 88.4 (SN, June 2013).

41.1% of the 1,807 OTUs produced by *uclust* and 76.3% of the 1,565 OTUs produced by CROP were assigned to Fungi, and the proportions assigned to each fungal class were similar across assignment methods (Table 1). Because we removed non-Fungi reads from the dataset before taxonomic assignment, we attribute the taxonomically unassigned OTUs to the still highly incomplete UNITE and Genbank databases used for taxonomic assignment.

Fungal diversity and CO₂ emissions – In June 2013, the month with the highest CO₂



emissions, emissions declined with fungal diversity in all wood species ($R^2 = 26\%$ to 44% , Fig. 1C, F).

In June 2012, CO₂ emissions from LC and SN also declined with fungal diversity, even though we used a fungal diversity estimate taken three months later (September 2012) and even after conservatively omitting an influential datum from SN (high CO₂, low diversity) (Fig. 1A, D). The third species (LX) did not return a significant regression, but its CO₂-diversity relationship was visually nearly indistinguishable from its congener LC, suggesting that wood species partly governs the emissions-diversity relationship. Variances explained (26% to 28%, Fig. 1A, D) were lower than in June 2013.

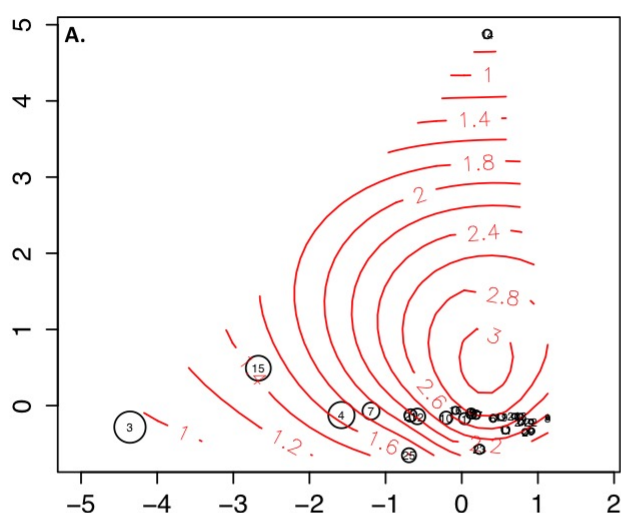
Finally, in September 2012, CO₂ emissions did not decline with higher fungal diversity (Fig. 1B, E), which is consistent with the generally lower CO₂ emissions in September (Fig. 1).

The above results were robust to two OTU-picking methods (CROP and *uclust*, Fig. 1), rarefaction (non-rarefied shown in Fig. 1; rarefied in Supporting Information S1), and two diversity estimates (Shannon in Fig. 1, Simpson in S1). Regressions using Simpson diversities were generally statistically *more* significant (S1). We also analyzed after omitting single-read OTUs (which are more likely to be pipeline artefacts²³) and achieved the same results, except that the previously non-significant SN regressions in Sept 2012 (Fig. 1A, D) became statistically *significant* (authors' unpublished results). In short, the analyses presented in Fig. 1 are conservative.

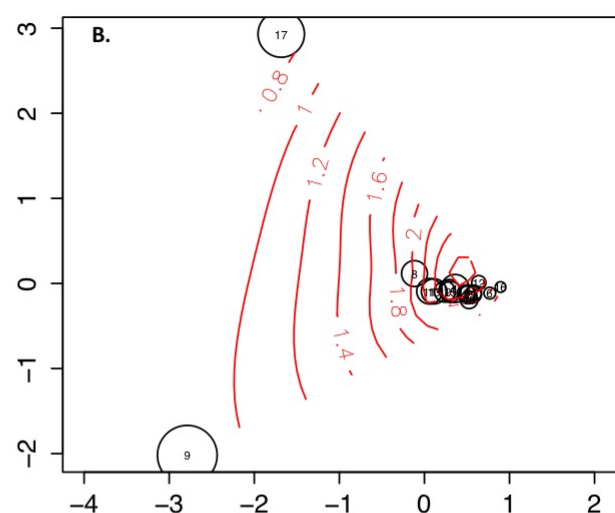
Chemistry of decomposing wood - We analyzed the chemistry of a separate subset of 27 wood pieces from the larger experiment. Mean CO₂ emissions from 2010-2012 showed no correlation with the densities of carbon, nitrogen, phosphorus, or lignin within any of the decay classes, with one exception, nitrogen density in decay class 1 (statistical details in Supporting Information S2).

Pure-diversity versus species-selection effects – Two general mechanisms could explain the observed diversity-function relationships. The first is a 'pure diversity' effect where species identity does not matter, only that increased species richness and evenness *per se* is somehow responsible for slower wood decomposition. The second is a 'species-selection' effect where more diverse fungal communities might be more likely to contain particular

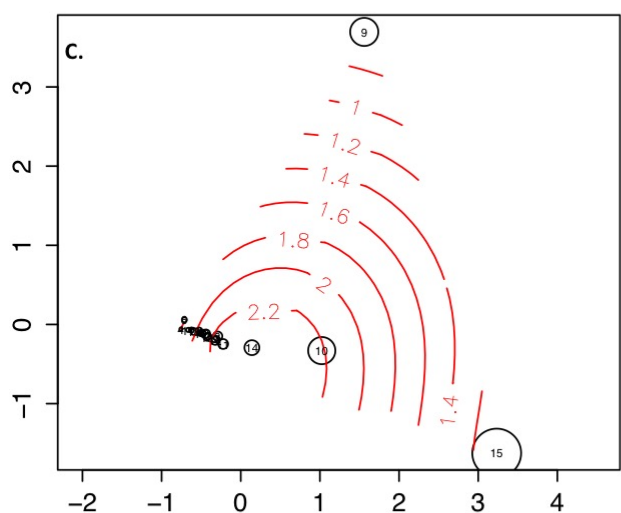
LC, June 2012 CO₂ ~ Sep 2012 Shannon



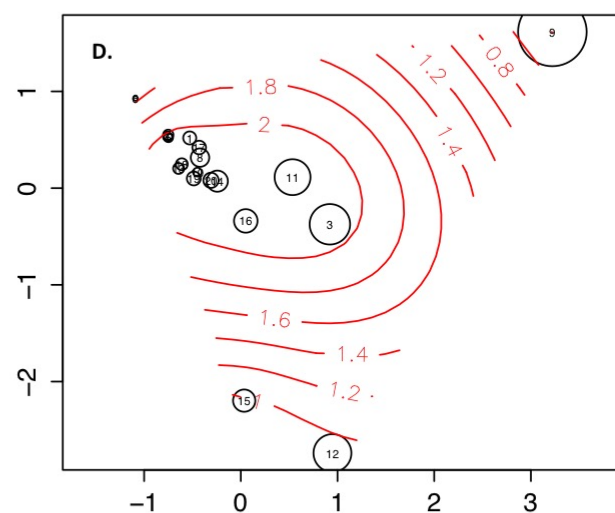
LC, June 2013 CO₂ ~ June 2013 Shannon



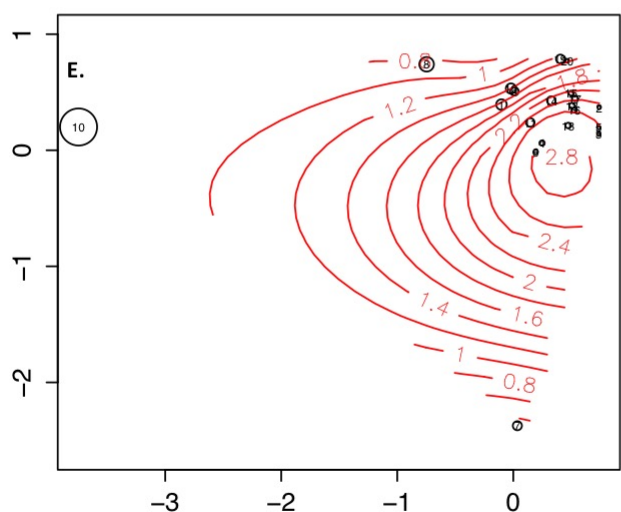
LX, June 2012 CO₂ ~ Sept 2012 Shannon



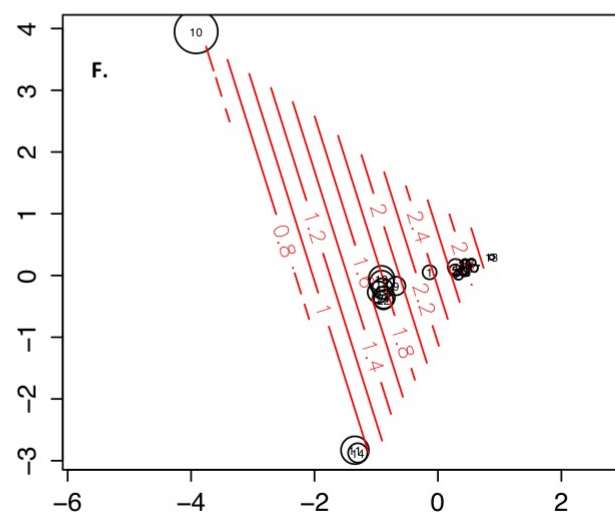
LX, June 2013 CO₂ ~ June 2013 Shannon



SN, June 2012 CO₂ ~ Sept 2012 Shannon



SN, June 2013 CO₂ ~ June 2013 Shannon



species that cause slow decomposition and somehow also govern the overall decomposition rate of the wood piece. To differentiate these two, we used a method devised by Sandau *et al.*²⁴ to generate a parameter λ for each regression in Fig. 1 (statistical details in Supporting Information S3). λ ranges between 0 and 1, with 0 indicating that variation in species composition does not account for variation in CO₂ emissions (i.e. a ‘pure-diversity’ effect). For two tree species, LC and LX, λ always took values near zero (Table 2). For the third tree species SN, λ was also nearly zero in June 2012 but took intermediate values in June 2013, suggesting that fungal composition in this tree species at this time had some explanatory power. The general failure to detect composition effects can be observed in the community ordinations (Fig. 2) by noting that the SN/June 2013 samples were the only ones to line up along the CO₂ emissions gradient (except the two lowest diversity samples). Not surprisingly, conventional community-analysis tests returned the same conclusion: variation in community composition is not explained by CO₂ emissions (statistical details in Supporting Information S4).

Discussion

We found that naturally colonised wood with more diverse fungal communities decomposes more slowly (Fig. 1), resulting in a negative relationship between fungal biodiversity and the ecosystem function of decomposition. This result suggests positive relationships between fungal biodiversity and the ecosystem services of carbon storage and the provision of decomposing-wood habitat in forests.

Our results are consistent with five published experiments using laboratory-inoculated wood, which have all found negative relationships between fungal diversity and decomposition rates^{10, 11, 12, 13, 25}. The one exception, Valentin *et al.*²⁶, found a positive relationship, but in that study, field-collected microbial communities were serially diluted and re-inoculated into laboratory wood incubations. Serial dilution does not necessarily remove microbial species, but it does make all species less abundant²⁷, which might have reduced decomposition rates.

In contrast, field studies to date have reported only ambiguous relationships between

fungal diversity and decomposition rates. For instance, Hoppe *et al.*²⁸ found non-significant correlations between fungal OTU richness and decay class (reflecting different numbers of years of decomposition), albeit negative relationships consistent with our results. Van Der Wal *et al.*²⁹ measured tree-stump decomposition and reported weakly *positive* effects of fungal species richness (but not Simpson diversity) on sapwood decomposition, but only in late decay. Kurbartová *et al.*³⁰ found no relationship between wood loss and fungal OTU diversity after 12 years of decomposition but also reported that the least-decayed logs had the highest community diversities, again consistent with our results. All three studies found differences in community composition for logs that differed in remaining undecomposed weights.

Importantly, none of those three field studies made concurrent measurements of fungal diversities and CO₂ emission rates, as we did here (Fig. 1). We observe that relationships between CO₂ emissions rate and fungal diversity varied from month to month and across tree species (Fig. 1, Table 2, S1), suggesting that fungal activity and composition are dynamic and environmentally responsive. Thus, the fungal community measured after years of decomposition might not reflect the communities that were active during decomposition, obscuring any relationship between mass loss and fungal diversity.

Our study helps to reconcile the differing results found in the published laboratory and field studies, by making concurrent measurements of emissions and fungal diversity in a field setting that is the most natural on the spectrum of possibilities: colonization of locally dominant tree species by the local fungal community, with uninterrupted and full exposure to local environmental variability and the local faunal community, including fungivores, and long-term succession of fungal and other microbial communities. Our collected wood pieces span a range of at least one to fifteen years of decomposition on the forest floor⁸. Our results suggest that laboratory experiments correctly reveal negative relationships between CO₂ emissions and fungal diversity.

Mechanisms. - In contrast to wood, microbial diversity is reported to accelerate the decomposition of soil organic matter^{31,32}, and this is thought to represent a general pattern^{33,34} (but see Creed *et al.*³⁵ for leaf litter). We hypothesise that because soil organic matter presents a much higher diversity of resources than does dead wood, niche complementarity amongst

decomposer species drives positive relationships between diversity and soil organic matter decomposition.

By contrast, niche overlap provides a plausible biological mechanism for why wood decomposition should *slow* with fungal diversity. Interference competition has long been predicted to evolve when niche overlap is high and the disputed resource is valuable³⁶. In forests, decomposing wood resources are available to many fungal species, and aggressive interactions are indeed observed among these fungi³⁷. Elsewhere, it has been shown that interference competition reduces virulence (= host consumption rate) in endosymbioses^{38,39,40} and productivity in bacterial communities^{41,42}. Consistent with those findings in other contexts, interference competition can also explain why fungal biomass has been found to explain variance in wood mass loss⁹. When a piece of wood is colonized by many fungal species, the hypothesized higher levels of interference competition would result in less wood converted into fungal biomass (or CO₂). High niche overlap is also consistent with the observed ‘pure diversity’ effect of fungal diversity on emissions (Table 2, S3, S4) since any species should fight all others (note, however, that we could not test for community composition effects at higher taxonomic levels, see Maherali & Klironomos⁴³). Thus, theory suggests that the arrow of causation can be drawn in the direction of fungal diversity driving decomposition rate. Finally, interference competition results in competitive exclusion, which will cause community composition to change over time. This means that measures of fungal diversity made after years of decomposition are unlikely to explain final variance in decomposition.

Sources of error and proposed future experiments. - One source of error is that metabarcoding provides only approximate estimates of species frequencies, due to the many errors known to be introduced by metabarcoding, especially PCR-primer mismatches that lead to biased amplification^{22, 23}. Also, DNA is environmentally persistent, so fungal species that are no longer represented by living colonies might still be detected by PCR. Nonetheless, we found that Shannon and Simpson indices, which both incorporate species frequency information by discounting rare species (here, rare=low-read OTUs), were able to explain variation in CO₂ emissions. There are two likely and non-exclusive explanations. (1) Low-read OTUs were more likely to have been the remains of dead species and/or sequence

artifacts from the metabarcoding pipeline and thus indeed should be discounted, and (2) in a Norway spruce forest, Ovaskainen *et al.*²¹ found that abundances of fungal fruiting bodies and OTU read numbers were positively correlated, suggesting that low-read OTUs indeed represent low-biomass species, which should have weaker influence on decomposition rates.

Another possible source of error is that we did not experimentally control for the age of the wood pieces, and thus an alternative explanation is that the observed correlations between fungal diversity and CO₂ emissions rates (Fig. 1) might be caused by sampling along a successional gradient in which older wood pieces have less remaining wood to decompose (and thus lower emissions) and have also accumulated more fungal species. However, we found no relationship between decay class and emissions rates (*Methods: Experimental setup and Statistical analyses*) in our dataset, nor did we in the 320-piece superset from which our samples were drawn⁸, whereas this alternative explanation predicts that the least-decayed wood pieces should show the highest emissions. Also, we found mostly ‘pure-diversity’ effects of fungal communities on emissions (Table 2, S3, S4), whereas this alternative explanation invokes a successional sere and thus predicts compositional effects. We suggest a long-term experiment in which even-aged and sterilized wood pieces are allowed to be colonized and sampled for CO₂ emissions rates and fungal diversity over many years in the field. We suggest that bacterial communities also be measured for correlations with CO₂ emissions, although we caution that to estimate alpha diversity, sequencing effort will need to be much higher than for fungal communities. In addition to DNA-based metabarcoding, it might also be informative to sequence reverse-transcribed RNA from wood samples, in order to isolate the effect of living fungal species.

Conclusions. - The slopes of our diversity-emissions relationships (Fig. 1) are steep enough to suggest that even modest declines in fungal diversity in dead wood could cause several-fold increases in CO₂ emissions rates. For example, in June 2013, CO₂ emissions varied by 5.6- and 14.4-fold among LC and LX wood pieces. These negative relationships between diversity and wood decomposition provide a strong justification to conduct large-scale surveys of the status of fungal biodiversity and its trajectories in the world’s forests. Global forest fragmentation, reduction of tree-species diversity by fires, logging and replanting, the removal of dead trees, and even increased rainfall could all reduce fungal

biodiversity in forests^{6,44}. All these changes could lead to faster wood decomposition. On the other hand, fragmented forests are drier, fungal distributions are being globalized⁴⁵, and their local diversity is increased by rising CO₂⁴⁶. The net effect of all these changes on carbon emissions from the world's stock of decomposing wood is difficult to predict.

Methods

Site description. – This study was conducted in the Ailao Mountains National Nature Reserve, Yunnan, China, which preserves the largest area of undisturbed, subtropical moist forest in China and has a substantial pool of woody debris (branches and logs, 74.9 x 10³ kg ha⁻¹, Ref. 47). The study site was at an elevation of 2476 m, about 2 km north of the Ailao Field Station for Forest Ecosystem Studies (24.533 °N, 101.017 °E), and receives 1840 mm annual average precipitation. The climate is monsoonal with distinct cool/dry (November to April) and warm/wet (May to October) seasons⁴⁸. Annual mean air temperature is 11.3 °C with monthly means ranging from 5 to 16 °C. Surface soils (0 to 10 cm) of the area are Alfisols with pH of 4.2 (in water). The surficial organic layer is 3 to 7 cm deep⁴⁹. The study site is a broad-leaved evergreen subtropical forest, with the canopy dominated by *Lithocarpus chintungensis*, *Rhododendron leptothrium*, *Vaccinium duchuoxii*, *Lithocarpus xylocarpus*, *Castanopsis wattii*, *Schima noronhae*, *Hartia sinensis*, and *Manglietia insignis*⁵⁰.

Experimental setup. – At our site, most woody debris comes from *Lithocarpus chintungensis*, (LC), *Lithocarpus xylocarpus* (LX), and *Schima noronhae* (SN), so we only examined those three species. In early 2010, branches from these three species, already decomposing on the forest floor, were identified to species by a botanist from the Xishuangbanna Tropical Botanical Garden, collected, and cut into a total of 320 wood pieces, sized to fit a field-respiration chamber (*ca.* 10 cm diameter and 20 to 30 cm length), tagged, weighed, and measured for size and decay class (further details in Liu *et al.*⁸). The three decay classes were DKC1 = a knife could not penetrate, DKC2 = a knife could slightly penetrate with appreciable resistance, DKC3 = a knife could deeply penetrate with little resistance⁵¹. We used similar-sized pieces to control for potential effects of wood size on fungal communities⁵². The pieces were placed on the forest floor within a 60 x 3 m belt

transect following an elevation contour. We collected source wood from within 500 m of this transect, utilizing about 5% of downed woody debris from these species in these decay classes, potentially arising from about 6000 source trees (D.A. Schaefer, unpublished data).

Each wood piece was initially weighed with a GLL portable electronic balance (accuracy 0.5 g) and for moisture content with an Extech MO210 moisture meter (calibrated as in Liu *et al.*⁸). Their volumes were calculated as cylinders, based on length and the average of 5 circumferential measurements along their lengths. From those, initial weight, volume, and density were all calculated. Oven drying of these wood pieces was not done, because it would have altered microbial communities and wood chemistry.

CO₂ emissions-rate measurements. – Individual wood-piece CO₂ release rates were measured in the field in a closed, ventilated chamber (10 L) connected to an infrared gas analyzer (Licor 820, Lincoln, NE, USA). After chamber closure and initial stabilization, linear CO₂ concentration increase rates were logged for at least 5 min. Pieces remained in the field for CO₂ measurements (within 5 m) and were handled carefully to limit fragmentation. Temperature and moisture were measured for each sample at each sampling time. The wood-piece CO₂ release rate (R_{WD} , $\mu\text{mol C g}^{-1} \text{ h}^{-1}$) was calculated as follows:

$$R_{WD} = (1000 * \Delta\text{CO}_2 * P * (V - V_s)) / (24 * R * (T_s + 273) * W_C) \quad (1)$$

where ΔCO_2 represents the measured CO₂ concentration increase (ppm day⁻¹), P is the internal pressure (kPa; measured by the Licor 820), V is the volume of the system (10.08 L, including the chamber volume and tubing volume and Licor optical path), V_s is the volume of the wood piece (L), R is the gas constant ($8.314 \text{ L}^{-1} \text{ kPa}^{-1} \text{ K}^{-1} \text{ mol}^{-1}$), T_s is the wood temperature (°C), and W_C is the carbon weight of each piece (g; 47% of its dry weight).

These measurements were made eight times from September 2010 to June 2013, approximately every four months (Fig. 1).

Sampling for genetic analysis. – The larger ongoing study includes three species, each having three decay classes, thus producing nine strata. 65 wood pieces were selected from all nine strata. In addition, for each stratum, we calculated a mean CO₂ emission rate during 2010-2012, and the pieces chosen for this experiment included ones that were consistently below, at, or above the mean rate, and also some that showed variation around the mean over time. Pieces for each of these subgroups were selected at random from the larger study. This

stratified random sampling ensured that all nine groups and the full range of CO₂ emission variation were represented in the metabarcoded samples. Those wood pieces were collected in September 2012, and 59 of those samples were recollected in June 2013 (6 samples were not relocated in June 2013, having lost their tags or been buried under new litter). We chose June and September because CO₂ emissions from wood are typically higher in June and lower in September, despite similarly warm temperatures and high moisture availability⁸ (Fig. 1 top). Superficial litter and bark were removed from each wood piece with a flame-sterilized knife before drilling. An electric drill with a flame-sterilized, 11-mm drill bit was used to extract wood powder at three holes located near the ends and the middle of each wood piece. Each sample consisted of ~5 cm³ pooled material from those three holes, collected onto aluminum-foil sheets, and then immediately stored in 50 ml tubes and frozen at -20 °C for 2-3 days until transport on ice packs to our laboratory 10 hr away, where they were stored at -40 °C until extractions.

Comparing cumulative CO₂ emissions and gravimetric weight losses. – Sixty-four additional wood pieces (*i.e.* not used for metabarcoding) were retrieved from the field in April 2013 to test the extent to which CO₂-emissions-estimated mass loss (averaged over the measurements taken from the year 2010 experiment start) accurately estimated directly measured mass loss (gravimetric weight loss). In the laboratory, these wood pieces were re-measured for volume (as above), and twenty-two wood pieces exhibiting >15% volumetric weight loss since the start of the experiment, indicating substantial fragmentation in the field, were excluded from the analysis. The remaining wood pieces were dried at 70 °C to constant weights and then individually weighed to the nearest 0.1 g on an electronic balance. CO₂-estimated mass loss was positively correlated with gravimetric loss (linear regression, Gravimetric loss in grams over 3 years = 30.7 + 0.741 * CO₂-based-decomposition Cd (R² = 0.769, n = 17, p <0.01); 28.7 + 0.56 * Cd (R² = 0.762, n = 13, p <0.01); and 40.3 + 0.468 * Cd (R² = 0.592, n = 13, p <0.01), for DKC1, 2, and 3, respectively. Inspection of scatterplots (Supporting Information S5) revealed that the main discrepancy was that CO₂-emission mass-loss estimates slightly underestimated small mass losses.

DNA extraction, PCR, and 454 pyrosequencing of ITS2 amplicons. – Total DNA was extracted from each sample of wood powder by adding 10 mL CTAB buffer (2% cetyl

trimethyl ammonium bromide, 50 mM NaCl, 5 mM EDTA, 10 mM Tris, pH 8) and 20 μ L β -mercaptoethanol per 5 cm³ of sample, homogenizing with a TH-02 homogenizer (Omni International, Kennesaw, GA USA) for 5 min at room temperature, incubating at 65 °C for 1 hour, centrifuging at 4,000 rpm for 1 min. After centrifugation, the supernatant was transferred to new Axygen® 2.0 mL microcentrifuge tubes and extracted using one volume of chloroform by vortexing for 20 min and centrifuged at 4 °C, 12,000 rpm for 10 min. The supernatant was then transferred to new microcentrifuge tubes and precipitated with 1.5 volumes of precooled isopropanol at -20 °C overnight. After centrifugation at 4 °C, 12,000 rpm for 20 min, the precipitate was washed with 70% ethanol and dissolved in 100 μ L TE buffer (10 mM Tris, 1 mM EDTA, pH 8.0). DNA was purified by using QIAquick PCR Purification Kit. The quantity and quality of purified DNA was assessed with a Nanodrop 2000 spectrophotometer (Thermo Fisher Scientific, Wilmington, DE, USA). Samples were PCR amplified using the forward primer ITS3_KYO2 5'-GATGAAGAACGYAGYRAA-3'¹⁸ and reverse primer ITS4 5'-TCCTCCGCTTATTGATATGC-3'⁵³. The standard Roche A-adaptor and a unique 10 bp MID (Multiplex Identifier) tag for each sample were attached to the forward primer. PCRs were performed using approximately 10 ng DNA in a 20 μ L reaction mixture containing 2 μ L of 10X buffer (Mg²⁺ Plus), 0.02 mM dNTPs, 20 μ g Bovine Serum Albumin, 1 μ L DMSO, 0.4 μ M of each primer, and 0.5 U HotStart Taq DNA polymerase (TaKaRa Biotechnology Co., Dalian, China) under a temperature profile of 95 °C for 10 min, followed by 35 cycles of 94 °C for 20 sec, 47 °C for 30 sec, and 72 °C for 2 min, and final extension at 72 °C for 7 min. For pyrosequencing, PCR products were gel-purified using Qiagen QIAquick PCR purification kit, quantified using the Quant-iT PicoGreen dsDNA Assay kit (Invitrogen, Grand Island, NY, USA), pooled and A-amplicon-sequenced on a Roche GS FLX (Branford, Connecticut, USA) at the Kunming Institute of Zoology.

Bioinformatic analyses. – The sequences obtained were run through a pipeline for quality control, denoising and chimera removal, OTU-picking and taxonomic assignment. Quality Control: Header sequences and low-quality reads were removed from the raw output in the QIIME 1.8.0 environment (*split_libraries.py*: -l 100 -L 500 -H 30)⁵⁴. The 65 samples collected in 2012 had been sequenced on four 1/8 regions, producing 679,361 raw reads and 525,679 post-quality-control reads (mean read length 286 bp). The 59 samples collected in

2013 had been sequenced on three 1/8 regions, producing 327,226 raw reads and 256,996 post-quality-control reads (mean read length 308 bp). These amplicon lengths were consistent with the expected mean length for ITS2 (327.2 bp, SD=40) reported by Toju *et al.*¹⁸.

Denoising and chimera removal: Denoiser in QIIME⁵⁵ was used to remove characteristic sequencing errors. Next, ITSx 1.0.3⁵⁶ was used to extract the variable ITS2 region from the whole reads (i.e. conserved 5.8S and LSU flanking sequences were stripped) and to remove non-fungal-ITS reads. The extracted sequences were clustered at 99% similarity with USEARCH v7.0.1090⁵⁷ to remove replicate sequences and chimeras. *OTU-picking and taxonomic assignment:* We used two methods to cluster the reads into OTUs. First, we used a reference-based method in QIIME (*pick_open_reference_otus.py*: max_accepts 20 max_rejects 500 stepwords 20 length 12 –suppress_align_and_tree) in which reads were first clustered by matching at 97% similarity to the UNITE 12_11 fungal database⁵⁸, which itself had previously been clustered at 97% similarity for use within QIIME. Unassigned reads (the vast majority) were then clustered *de novo* using the *uclust* option at 97% similarity, producing 1,807 OTUs in total. For these latter OTUs, we attempted to assign taxonomies using QIIME's *assign_taxonomy.py* against the UNITE database. Second, we performed *de novo* 97%-similarity clustering with CROP 1.33⁵⁹, producing 1,565 OTUs. We assigned taxonomies against Genbank using the NNCauto and QCauto methods in Claident⁶⁰.

Sequence data are deposited at datadryad.org (doi: to be assigned) and in GENBANK's Short Read Archive (Accession number: PRJNA252416). An example bioinformatic script is in Supplementary Information and also deposited at datadryad.org (doi: to be assigned).

Statistical analyses. – Analyses were performed using *vegan* 2.0-10⁶¹ and *mvabund* 3.8.4⁶² in R 3.1.0⁶³. The HTML outputs of the R scripts are in Supplementary Information and also deposited at datadryad.org (doi: to be assigned). From both the OTU tables generated (CROP and *uclust*, see *Bioinformatic analysis*), we deleted one SN wood piece that had only 35 reads and then split the tables by wood species (LC, LX, and SN) and sample time (September 2012 and June 2013). We then generated a second pair of OTU tables by rarefying to the lowest read number per wood piece in the dataset (*rrarefy()* in R). Thus, for each wood species and sampling time, we have four OTU tables: CROP/non-rarefied, CROP/rarefied, *uclust*/non-rarefied, and *uclust*/rarefied. Finally, for each table, we used

378 *vegan*'s *diversity()* function to estimate Shannon and Simpson diversity in each wood piece.

379 For each wood species, we used *lm()* in *R* to linearly regress emissions against fungal
380 diversity. Thus, the June 2012 and September 2012 CO₂ estimates were tested against the
381 September 2012 fungal diversity estimate, and the June 2013 CO₂ estimate was tested against
382 the June 2013 fungal diversity estimate. Residuals were all adjudged visually to be near
383 normally distributed, but with small indications of nonlinearity. We ignored the nonlinearities
384 because the residuals suggested accelerating CO₂ emissions at the lowest fungal diversity,
385 making our results conservative. In trial models, we also tested for significant effects of wood
386 surface temperature and decay class (see *Experimental setup*), but they did not interact
387 significantly with the fungal diversity term and mostly did not enter significantly as additive
388 terms, and so have been omitted here for simplicity. Liu *et al.*⁸ also did not find a correlation
389 between decay class and CO₂ emissions rates for these wood pieces.

390 To test whether a 'pure diversity' effect is sufficient to explain the observed
391 diversity-function relationships, we use a method by Sandau *et al.*²⁴ where community
392 similarities (1-Jaccard binary) between all wood pieces are used to create a
393 variance-covariance matrix that is then included in the linear regressions, thus taking into
394 account potential non-independence of wood pieces due to the fact that some communities
395 are similar to each other (Supporting Information S3). In Supporting Information S4, we also
396 use conventional community analyses to test for an effect of community composition on CO₂
397 emissions. We limit our tests to June 2012 and 2013, as only these exhibited significant
398 declines in emissions with fungal-species diversity (Fig. 1A, C, D, F).

399 References

- 400 1. Matthews, E. Global litter production, pools, and turnover times: estimates from measurement data
401 and regression models. *J. Geophys. Res.* **102**, 18771–18800 (1997).
- 402 2. Harmon, M. E., Krankina, O. N., Yatskov, M. & Matthews, E. Predicting broad-scale carbon stores
403 of woody detritus from plot-level data in *Assessment Methods for Soil Carbon* (eds. Lal, R.,
404 Kimble, J. & Stewart, B. A.) 533–552 (CRC Press, 2001).
- 405 3. Luyssaert, S. *et al.* CO₂ balance of boreal, temperate, and tropical forests derived from a global
406 database. *Glob. Change Biol.* **13**, 2509–2537 doi:10.1111/j.1365-2486.2007.01439.x (2007).
- 407 4. Le Quéré, C. *et al.* The global carbon budget 1959–2011. *Earth Syst. Sci. Data* **5**, 165–185

- doi:10.5194/essd-5-165-2013 (2013).
5. Lindenmayer, D. B. *et al.* A major shift to the retention approach for forestry can help resolve some global forest sustainability issues. *Conserv. Lett.* **5**, 421–431 doi:10.1111/j.1755-263X.2012.00257.x (2012).
6. Stokland, J.N., Siitonen, J. & Jonsson, B.G. *Biodiversity in Dead Wood*. (Cambridge University Press, 2012)
7. Chambers, J. Q., Schimel, J. P. & Nobre, A. D. Respiration from coarse wood litter in central Amazon forests. *Biogeochemistry* **52**, 115–131 (2001).
8. Liu, W., Schaefer, D., Qiao, L. & Liu, X. What controls the variability of wood-decay rates? *For. Ecol. Manage.* **310**, 623–631 doi:10.1016/j.foreco.2013.09.013 (2013).
9. Bradford, M. A. *et al.* Climate fails to predict wood decomposition at regional scales. *Nature Clim. Change* **4**, 625–630 doi:10.1038/nclimate2251 (2014).
10. Toljander, Y. K., Lindahl, B. D., Holmer, L. & Högborg, N. O. S. Environmental fluctuations facilitate species co-existence and increase decomposition in communities of wood decay fungi. *Oecologia* **148**, 625–631 doi:10.1007/s00442-006-0406-3 (2006).
11. Fukami, T. *et al.* Assembly history dictates ecosystem functioning: evidence from wood decomposer communities. *Ecol. Lett.* **13**, 675–684 doi:10.1111/j.1461-0248.2010.01465.x (2010).
12. Lindner, D. L. *et al.* Initial fungal colonizer affects mass loss and fungal community development in *Picea abies* logs 6 yr after inoculation. *Fungal Ecol.* **4**, 449–460 doi:10.1016/j.funeco.2011.07.001 (2011).
13. Peay, K. G., Dickie, I. A., Wardle, D. A., Bellingham, P. J. & Fukami, T. Rat invasion of islands alters fungal community structure, but not wood decomposition rates. *Oikos* **122**, 258–264 doi:10.1111/j.1600-0706.2012.20813.x (2013).
14. Tordoff, G. M., Boddy, L. & Jones, T. H. Species-specific impacts of collembolan grazing on fungal foraging ecology. *Soil Biol. Biochem.* **40**, 434–442 doi:10.1016/j.soilbio.2007.09.006 (2008).
15. Crowther, T. W., Boddy, L. & Jones, T. H. Outcomes of fungal interactions are determined by soil invertebrate grazers. *Ecol. Lett.* **14**, 1134–1142 doi:10.1111/j.1461-0248.2011.01682.x (2011).
16. A’Bear, A. D., Boddy, L. & Jones, T. H. Impacts of elevated temperature on the growth and functioning of decomposer fungi are influenced by grazing Collembola. *Glob. Change Biol.* **18**, 1823–1832 doi:10.1111/j.1365-2486.2012.02637.x (2012).
17. Ji, Y. *et al.* Reliable, verifiable and efficient monitoring of biodiversity via metabarcoding. *Ecol. Lett.* **16**, 1245–1257 doi:10.1111/ele.12162 (2013).
18. Toju, H., Tanabe, A. S., Yamamoto, S. & Sato, H. High-coverage ITS primers for the DNA-based identification of Ascomycetes and Basidiomycetes in environmental samples. *PLoS ONE* **7**(7), e40863 doi:10.1371/journal.pone.0040863.t004 (2012).
19. Bazzicalupo, A. L., Bálint, M. & Schmitt, I. Comparison of ITS1 and ITS2 rDNA in 454 sequencing of hyperdiverse fungal communities. *Fungal Ecol.* **6**, 102–109 doi:10.1016/j.funeco.2012.09.003 (2013)

20. Lindahl, B. D. *et al.* Fungal community analysis by high-throughput sequencing of amplified markers - a user's guide. *New Phytol.* **199**, 288–299. doi:10.1111/nph.12243 (2013).
21. Ovaskainen, O. *et al.* Combining high-throughput sequencing with fruit body surveys reveals contrasting life-history strategies in fungi. *ISME J.* **7**, 1696–1709 doi:10.1038/ismej.2013.61 (2013).
22. Amend, A. S., Seifert, K. A. & Bruns, T. D. Quantifying microbial communities with pyrosequencing: does read abundance count? *Mol. Ecol.* **19**, 5555–5565 doi:10.1111/j.1365-294X.2010.04898.x (2010).
23. Yu, D. *et al.* Biodiversity soup: metabarcoding of arthropods for rapid biodiversity assessment and biomonitoring. *Methods Ecol. Evol.* **3**, 613–623 doi:10.1111/j.2041-210X.2012.00198.x (2012).
24. Sandau, N. *et al.* Including community composition in biodiversity-productivity models. *Methods Ecol. Evol.* **5**, 815–823 doi: 10.1111/2041-210X.12215 (2014).
25. Dickie, I. A., Fukami, T., Wilkie, J. P., Allen, R. B. & Buchanan, P.K. Do assembly history effects attenuate from species to ecosystem properties? A field test with wood-inhabiting fungi. *Ecol. Lett.* **15**, 133–141 doi:10.1111/j.1461-0248.2011.01722.x (2012).
26. Valentín, L. *et al.* Loss of diversity in wood-inhabiting fungal communities affects decomposition activity in Norway spruce wood. *Front. Microbiol.* **5**, 230 doi: 10.3389/fmicb.2014.00230 (2014).
27. Yan, Y., Kuramae, E. E., Klinkhamer, P. G. L. & van Veen, J. A. The dilution procedure to manipulate microbial biodiversity in terrestrial systems revisited. *Appl. Environ. Microbiol.* **81**, 4246–4251 doi: 10.1128/AEM.00958-15 (2015).
28. Hoppe, B., *et al.* Linking molecular deadwood-inhabiting fungal diversity and community dynamics to ecosystem functions and processes in Central European forests. *Fung. Divers.*, doi:10.1007/s13225-015-0341-x (2015).
29. Van Der Wal, A., Ottosson, E. & De Boer, W. Neglected role of fungal community composition in explaining variation in wood decay rates. *Ecology* **96**, 124–133 doi:10.1890/14-0242.1 (2015).
30. Kubartová, A., Ottosson, E. & Stenlid, J. Linking fungal communities to wood density loss after 12 years of log decay. *FEMS Microbiol. Ecol.* **91** doi: 10.1093/femsec/fiv032 (2015).
31. Nielsen, U. N., Ayres, E., Wall, D. H. & Bardgett, R. D. Soil biodiversity and carbon cycling: a review and synthesis of studies examining diversity–function relationships. *Eur. J. Soil Sci.* **62**, 105–116 doi:10.1111/j.1365-2389.2010.01314.x (2011).
32. Baumann, K. *et al.* Soil microbial diversity affects soil organic matter decomposition in a silty grassland soil. *Biogeochemistry* **114**, 201–212 doi:10.1007/s10533-012-9800-6 (2013).
33. Gessner, M. O. *et al.* Diversity meets decomposition. *Trends Ecol. Evol.* **25**, 372–380 doi:10.1016/j.tree.2010.01.010 (2010).
34. van der Wal, A., Geydan, T. D., Kuyper, T. W. & de Boer, W. A thready affair: linking fungal diversity and community dynamics to terrestrial decomposition processes. *FEMS Microbiol. Rev.* **37**, 477–494 doi:10.1111/1574-6976.12001 (2013).
35. Creed, R. P., Cherry, R. P., Pflaum, J. R. & Wood, C. J. Dominant species can produce a negative relationship between species diversity and ecosystem function. *Oikos*, **118**, 723–732

- doi:10.1111/j.1600-0706.2008.17212.x (2009).
36. Case T. & Gilpin, M. Interference competition and niche theory. *Proc. Natl. Acad. Sci USA.*, **71**, 3073–3077 (1974).
37. Woodward, S. & Boddy, L. Interactions between saprotrophic fungi in *Ecology of Saprotrophic Basidiomycetes* (eds. Boddy, L., Frankland, J. C. & van West, P.) 124–139 (Elsevier, 2008)
38. Massey, R. C., Buckling, A. & Ffrench-Constant, R. Interference competition and parasite virulence. *Proc. R. Soc. B. Biol. Sci.* **271**, 785–788 doi:10.1098/rspb.2004.2676.S (2004)
39. Vigneux, F., Bashey, F., Sicard, M. & Lively, C. M. Low migration decreases interference competition among parasites and increases virulence. *J. Evol. Biol.* **21**, 1245–1251 doi:10.1111/j.1420-9101.2008.01576.x (2008).
40. Wang, R. W. *et al.* Interference competition and high temperatures reduce the virulence of fig wasps and stabilize a fig-wasp mutualism. *PLoS ONE* **4**, e7802 doi:10.1371/journal.pone.0007802 (2009).
41. Foster, K. R. & Bell, T. Competition, not cooperation, dominates interactions among culturable microbial species. *Curr. Biol.* **22**, 1845–1850 doi:10.1016/j.cub.2012.08.005 (2012).
42. Becker, J., Eisenhauer, N., Scheu, S. & Jousset, A. Increasing antagonistic interactions cause bacterial communities to collapse at high diversity. *Ecol. Lett.* **15**, 468–474 doi:10.1111/j.1461-0248.2012.01759.x (2012).
43. Maherali, H. & Klironomos, J. N. Influence of phylogeny on fungal community assembly and ecosystem functioning. *Science* **316**, 1746–1748 doi:10.1126/science.1143082 (2007).
44. Hawkes, C. V. *et al.* Fungal community responses to precipitation. *Glob. Change Biol.* **17**, 1637–1645 doi:10.1111/j.1365-2486.2010.02327.x (2011).
45. Bebbler, D. P., Holme, T. & Gurr, S. J. The global spread of crop pests and pathogens. *Glob. Ecol. Biogeogr.* **23**, 1398–1407 doi:10.1111/geb.12214 (2014).
46. Lipson, D. A., Kuske, C. R., Gallegos-Graves, L. & Oechel, W. C. Elevated atmospheric CO₂ stimulates soil fungal diversity through increased fine root production in a semiarid shrubland ecosystem. *Glob. Change Biol.* **20**, 2555–2565 doi:10.1111/gcb.12609 (2014).
47. Yang, L. P., Liu, W. Y. & Ma, W. Z. Woody debris stocks in different secondary and primary forests in the subtropical Ailao Mountains, southwest China. *Ecol. Res.* **23**, 805–812 doi:10.1007/s11284-007-0442-4 (2008).
48. Zhang, K. The characteristics of mountain climate in the North of Ailao Mts. in *Research of Forest Ecosystem on Ailao Mountains, Yunnan* (eds. Wu, Z. Y., Qu, Z. X. & Jiang, H.Q.) 20–29 (Yunnan Science and Technology Press, 1983).
49. Liu, W. Y., Fox, J. E. D. & Xu, Z. F. Biomass and nutrient accumulation in montane evergreen broad-leaved forest (*Lithocarpus xylocarpus* type) in Ailao Mountains, SW China. *For. Ecol. Manage.* **158**, 223–235 (2002).
50. Wu, Z. Y., Qu, Z. X. & Jiang, H. Q. *Research of Forest Ecosystem on Ailao Mountains, Yunnan* (Yunnan Science and Technology Press, 1983).
51. Lambert, R. L., Lang, G. E. & Reiners, W. A. Loss of mass and chemical change in decaying boles

- of a subalpine fir forest. *Ecology* **61**, 1460–1473 (1980).
52. Juutilainen, K., Halme, P., Kotiranta, H. & Mönkkönen, M. Size matters in studies of dead wood and wood-inhabiting fungi. *Fungal Ecol.* **4**, 342–349 doi:10.1016/j.funeco.2011.05.004 (2011).
53. White, T. J., Bruns, T., Lee, S. & Taylor, J. Amplification and direct sequencing of fungal ribosomal RNA genes for phylogenetics in *PCR Protocols. A Guide to Methods and Applications* (eds. Innis, M. A., Gelfand, D. H., Sninsky, J. J. & White, T. J.) 315–322 (Academic Press, 1990).
54. Caporaso, J. G. *et al.* QIIME allows analysis of high-throughput community sequencing data. *Nature Methods* **7**, 335–336 doi:10.1038/nmeth.f.303 (2010).
55. Reeder, J. & Knight, R. Rapidly denoising pyrosequencing amplicon reads by exploiting rank-abundance distributions. *Nature Methods* **7**, 668–669 doi:10.1038/nmeth0910-668b (2010).
56. Bengtsson-Palme, J. *et al.* Improved software detection and extraction of ITS1 and ITS2 from ribosomal ITS sequences of fungi and other eukaryotes for analysis of environmental sequencing data. *Methods Ecol. Evol.* **4**, 914–919 doi:10.1111/2041-210X.12073 (2013).
57. Edgar, R. C. Search and clustering orders of magnitude faster than BLAST. *Bioinformatics* **26**, 2460–2461 doi:10.1093/bioinformatics/btq461 (2010).
58. Kõljalg, U. *et al.* Towards a unified paradigm for sequence-based identification of fungi. *Mol. Ecol.* **22**, 5271–5277 doi:10.1111/mec.12481 (2013).
59. Hao, X., Jiang, R. & Chen, T. Clustering 16S rRNA for OTU prediction: a method of unsupervised Bayesian clustering. *Bioinformatics* **27**, 611–618 doi:10.1093/bioinformatics/btq725 (2011).
- 60 Tanabe, A. S. & Toju, H. Two new computational methods for universal DNA barcoding: a benchmark using barcode sequences of bacteria, Archaea, animals, fungi, and land plants. *PLoS ONE* **8**, e76910 doi:10.1371/journal.pone.0076910 (2013).
61. Oksanen, J. *et al.* (2013) *vegan*: Community Ecology R package. URL <http://CRAN.R-project.org/package=vegan>. (Accessed: 30th May 2014).
62. Warton, D. I., Wright, S. T. & Wang, Y. Distance-based multivariate analyses confound location and dispersion effects. *Methods Ecol. Evol.* **3**, 89–101 doi:10.1111/j.2041-210X.2011.00127.x (2014).
63. R Core Team (2014). *R*: A language and environment for statistical computing. R Foundation for Statistical Computing, Vienna, Austria. URL <http://www.R-project.org/>.

Acknowledgments

We thank our two reviewers for their very helpful suggestions. CYY, DWY, CXY, XYW and CYW were supported by Yunnan Province (20080A001), the Chinese Academy of Sciences (0902281081, KSCX2-YW-Z-1027), the National Natural Science Foundation of China (31400470, 31170498), the Ministry of Science and Technology of China (2012FY110800), the University of East Anglia, and the State Key Laboratory of Genetic Resources and Evolution at the Kunming Institute of Zoology. DAS and WJL were supported by the

Asia-Pacific Network for Global Change Research (ARCP 2009-18MY), the National Natural Science Foundation of China (30970535 and 41271278), the Chinese Academy of Sciences 135 program (XTBG-T01), and the Xishuangbanna Tropical Botanical Garden. Zhang Yiping provided Ailao Mountain meteorological data; Yang Gunping identified the wood pieces; Qiao Lu and Liu Xianbin assisted in the field work.

Author contributions

DAS, CYY, and DWY designed the study. CYY, WJL and DAS carried out the field work. CYY, CXY, XYW and CYW performed the DNA analyses. CYY and DWY carried out the bioinformatics. DWY and VP carried out the statistical analyses. DWY, DAS and CYY wrote the first draft. WJL and CXY commented on the manuscript.

Additional information

DWY is co-founder of a UK company, NatureMetrics, which provides DNA metabarcoding services to the private and public sector. All other authors declare no conflicts of interest.

Figure legends

Figure 1. Linear regressions of CO₂ emission rates on Shannon fungal diversities measured from individually metabarcoded wood pieces. **Top.** The solid black curve indicates the air temperature. Carets indicate times of CO₂ measurements. Blue shading indicates the warm months when wood decomposition is >50% of maximum. **A-C.** CO₂ emissions decline with increased fungal species diversity in two of the species in June 2012 (LC and SN) and in all three species in June 2013. In September 2012, CO₂ emissions are lower, and there is no relationship. The OTU-picking method is *de novo* clustering with CROP. **D-F.** Same as A-C but the OTU-picking method is QIIME's reference-based matching against the UNITE database, with *de novo* clustering of non-matched reads with *uclust*. Non-significant regressions are indicated by dashed lines. Shown here are the non-rarefied datasets. Rarefaction does not change the results (Supporting Information S1). LC = *Lithocarpus chintungensis*, LX = *L. xylocarpus*, SN = *Schima noronhae*.

Figure 2. Correspondence analysis ordinations of fungal communities, by tree species and sampling date. Point size is scaled to CO₂ emissions, and the gradient represents fungal Shannon diversity. In all ordinations (**A-F**), CO₂ emissions decrease with higher fungal diversity (point size decreases up the gradient, echoing Fig. 1). Also evident is that the lower diversity wood pieces are compositionally very dissimilar to each other and to the higher diversity wood pieces. **Left-hand column (A, C, E).** June 2012 CO₂ vs. September 2012 fungal diversity. **Right-hand column (B, D, F).** June 2013 CO₂ vs. June 2013 fungal diversity. **A-B.** *Lithocarpus chintungensis*. Note that the label for point 14 at the top of A is obscured by the small point size. **C-D.** *L. xylocarpus*. **E-F.** *Schima noronhae*. Shown here are the non-rarefied datasets clustered using CROP (see Methods). Rarefaction or using *uclust*-clustering does not change the results (Supporting Information S4).

Tables

Table 1. Taxonomic assignments to Class level for the ITS2 Operational Taxonomic Units (OTUs). *uclust* and CROP refer to the two OTU-clustering methods used, and GenBank and UNITE refer to the fungal reference databases used (see Methods: *Bioinformatic Analyses* for details).

CROP + Genbank (1,565 OTUs)							
Kingdom Fungi	Ascomycota	Basidiomycota	Chytridiomycota	Zygomycota	Glomeromycota	Mortierellales	Phylum unidentified
1194 OTUs	632	319	1	3	1	3	235
76.3% of total	52.9% of Fungi	26.70%	0.10%	0.30%	0.10%	0.30%	19.70%
<i>uclust</i> + UNITE (1,806 OTUs)							
Kingdom Fungi	Ascomycota	Basidiomycota	Chytridiomycota	Zygomycota	Phylum unidentified		
742 OTUs	378	169	2	5	188		
41.1% of total	50.9% of Fungi	22.80%	0.30%	0.70%	25.30%		

Table 2. Estimates of the contribution of fungal community composition to CO₂ emissions, using the method of Sandau *et al.*²⁴. The generated parameter λ varies between 0 and 1, with 0 indicating that variation in composition does not explain variation in emissions. Composition only contributes to explaining variation in one tree species in one sampling date (SN, June 2013). Conventional community analysis (Supporting Information S4) also detected a contribution of composition in SN in June 2013. LC = *Lithocarpus chintungensis*, LX = *L. xylocarpus*, SN = *Schima noronhae*.

CO ₂ sample	Species	OTU clustering	λ
Jun-12	LC	CROP	0.000
		<i>uclust</i>	0.000
	LX	CROP	0.002
		<i>uclust</i>	0.000
	SN	CROP	0.001
		<i>uclust</i>	0.004
Jun-13	LC	CROP	0.000
		<i>uclust</i>	0.000
	LX	CROP	0.000
		<i>uclust</i>	0.001
	SN	CROP	0.366
		<i>uclust</i>	0.500

Higher fungal diversity is correlated with lower CO₂ emissions from dead wood in a natural forest:

Supplementary Information

Chunyan Yang^{1,*}, Douglas A. Schaefer^{2,*}, Weijie Liu², Viorel D. Popescu³,
Chenxue Yang¹, Xiaoyang Wang¹, Chunying Wu¹, Douglas W. Yu^{1,4,**}

¹ State Key Laboratory of Genetic Resources and Evolution, Kunming Institute of Zoology, Chinese Academy of Sciences, 32 Jiaochang East Rd., Kunming, Yunnan 650223 China

² Key Laboratory of Tropical Forest Ecology, Chinese Academy of Sciences, Xishuangbanna Tropical Botanical Garden, Menglun, Mengla, Yunnan 666303, China

³ Earth to Ocean Research Group, Department of Biological Sciences, Simon Fraser University, Burnaby, British Columbia V5A1S6, Canada

⁴ School of Biological Sciences, University of East Anglia, Norwich Research Park, Norwich, Norfolk NR47TJ UK

* These authors contributed equally.

** Corresponding author: tel: +4407510308272 and +8618608717369; fax: +441603592250; emails: dougwyu@gmail.com and douglas.yu@uea.ac.uk; Twitter: @insectsoup

Higher fungal diversity is correlated with lower CO₂ emissions from dead wood in a natural forest:

S1 Summary of Regression Analyses

S1 Summary of Regression analyses

OTU-pickng	rarefaction	CO2 measurement	species	diversity	p-value	notes
CROP	nonrarefied	Jun-12	LC	Shannon	0.007	
CROP	nonrarefied	Jun-12	LC	Simpson	0.015	
CROP	nonrarefied	Jun-12	LX	Shannon	0.080	
CROP	nonrarefied	Jun-12	LX	Simpson	0.040	
CROP	nonrarefied	Jun-12	SN	Shannon	0.027	removed influential woodpiece=110
CROP	nonrarefied	Jun-12	SN	Simpson	0.018	removed influential woodpiece=110
CROP	nonrarefied	Sep-12	LC	Shannon	0.460	
CROP	nonrarefied	Sep-12	LC	Simpson	0.642	
CROP	nonrarefied	Sep-12	LX	Shannon	0.116	
CROP	nonrarefied	Sep-12	LX	Simpson	0.057	
CROP	nonrarefied	Sep-12	SN	Shannon	0.700	
CROP	nonrarefied	Sep-12	SN	Simpson	0.474	
CROP	nonrarefied	Jun-13	LC	Shannon	0.003	
CROP	nonrarefied	Jun-13	LC	Simpson	0.000	
CROP	nonrarefied	Jun-13	LX	Shannon	0.025	
CROP	nonrarefied	Jun-13	LX	Simpson	0.016	
CROP	nonrarefied	Jun-13	SN	Shannon	0.003	
CROP	nonrarefied	Jun-13	SN	Simpson	0.001	
CROP	rarefied	Jun-12	LC	Shannon	0.005	
CROP	rarefied	Jun-12	LC	Simpson	0.014	
CROP	rarefied	Jun-12	LX	Shannon	0.084	
CROP	rarefied	Jun-12	LX	Simpson	0.044	
CROP	rarefied	Jun-12	SN	Shannon	0.020	removed influential woodpiece=110
CROP	rarefied	Jun-12	SN	Simpson	0.037	removed influential woodpiece=110
CROP	rarefied	Sep-12	LC	Shannon	0.563	
CROP	rarefied	Sep-12	LC	Simpson	0.572	

The (bolded) Shannon results from this first section are plotted in Fig. 1A-C.

CROP	rarefied	Sep-12 LX	Shannon	0.123	
CROP	rarefied	Sep-12 LX	Simpson	0.062	
CROP	rarefied	Sep-12 SN	Shannon	0.693	
CROP	rarefied	Sep-12 SN	Simpson	0.475	
CROP	rarefied	Jun-13 LC	Shannon	0.004	
CROP	rarefied	Jun-13 LC	Simpson	0.001	
CROP	rarefied	Jun-13 LX	Shannon	0.030	
CROP	rarefied	Jun-13 LX	Simpson	0.019	
CROP	rarefied	Jun-13 SN	Shannon	0.004	
CROP	rarefied	Jun-13 SN	Simpson	0.001	
uclust	nonrarefied	Jun-12 LC	Shannon	0.003	
uclust	nonrarefied	Jun-12 LC	Simpson	0.005	
uclust	nonrarefied	Jun-12 LX	Shannon	0.086	
uclust	nonrarefied	Jun-12 LX	Simpson	0.044	
uclust	nonrarefied	Jun-12 SN	Shannon	0.538	removed influential woodpiece=110
uclust	nonrarefied	Jun-12 SN	Simpson	0.439	removed influential woodpiece=110
uclust	nonrarefied	Sep-12 LC	Shannon	0.499	
uclust	nonrarefied	Sep-12 LC	Simpson	0.593	
uclust	nonrarefied	Sep-12 LX	Shannon	0.138	
uclust	nonrarefied	Sep-12 LX	Simpson	0.066	
uclust	nonrarefied	Sep-12 SN	Shannon	0.500	
uclust	nonrarefied	Sep-12 SN	Simpson	0.265	
uclust	nonrarefied	Jun-13 LC	Shannon	0.003	
uclust	nonrarefied	Jun-13 LC	Simpson	0.000	
uclust	nonrarefied	Jun-13 LX	Shannon	0.028	
uclust	nonrarefied	Jun-13 LX	Simpson	0.018	
uclust	nonrarefied	Jun-13 SN	Shannon	0.004	
uclust	nonrarefied	Jun-13 SN	Simpson	0.001	

The (bolded) Shannon results from this
thrd section are plotted in Fig. 1D-F.

uclust	rarefied	Jun-12 LC	Shannon	0.005	
uclust	rarefied	Jun-12 LC	Simpson	0.003	
uclust	rarefied	Jun-12 LX	Shannon	0.094	
uclust	rarefied	Jun-12 LX	Simpson	0.049	
uclust	rarefied	Jun-12 SN	Shannon	0.096	removed influential woodpiece=110
uclust	rarefied	Jun-12 SN	Simpson	0.144	removed influential woodpiece=110
uclust	rarefied	Sep-12 LC	Shannon	0.441	
uclust	rarefied	Sep-12 LC	Simpson	0.590	
uclust	rarefied	Sep-12 LX	Shannon	0.136	
uclust	rarefied	Sep-12 LX	Simpson	0.066	
uclust	rarefied	Sep-12 SN	Shannon	0.482	
uclust	rarefied	Sep-12 SN	Simpson	0.247	
uclust	rarefied	Jun-13 LC	Shannon	0.004	
uclust	rarefied	Jun-13 LC	Simpson	0.001	
uclust	rarefied	Jun-13 LX	Shannon	0.026	
uclust	rarefied	Jun-13 LX	Simpson	0.018	
uclust	rarefied	Jun-13 SN	Shannon	0.004	
uclust	rarefied	Jun-13 SN	Simpson	0.001	

Higher fungal diversity is correlated with lower CO₂ emissions from dead wood in a natural forest:

S2 Wood chemistry analyses

Supporting Information S2. Wood chemistry analyses.

Methods

In January 2013, 27 decaying wood samples from our larger study were removed from the field for chemical analyses. Included were 3 pieces from each combination of wood species (LC, LX, and SN) and decay class (DKC 1, 2, 3), spanning the range of previously observed decomposition rates. These pieces were dried at 60 °C to constant weights and milled to pass a 40 mesh (425 micron opening) sieve. They were analyzed for total carbon and nitrogen (Macro Elemental CN Analyzer, Vario MAX CN, Germany), for total phosphorus (continuous Flow Analyzer, Auto Analyzer 3, Germany) after acid digestion, and for lignin (Fibertec 2010 System, Fibertec, Denmark). The metabarcoded wood pieces remain in the field and were not analyzed.

Column headings explanation

Tag: Permanent identification number assigned to each piece of wood in this study

Tree_species: LC = *Lithocarpus chintungensis*, LX = *Lithocarpus xylocarpus* (LX), and SN = *Schima noronhae*

Average_CO₂: CO₂ release rate for each wood piece from 2010 to 2012, average of 6 measurements, micromoles CO₂ per dry gram of wood carbon per hour

Total_carbon_g/kg: Carbon as grams per dry kilogram of wood weight

Total_Nitrogen_g/kg: Nitrogen as grams per dry kilogram of wood weight

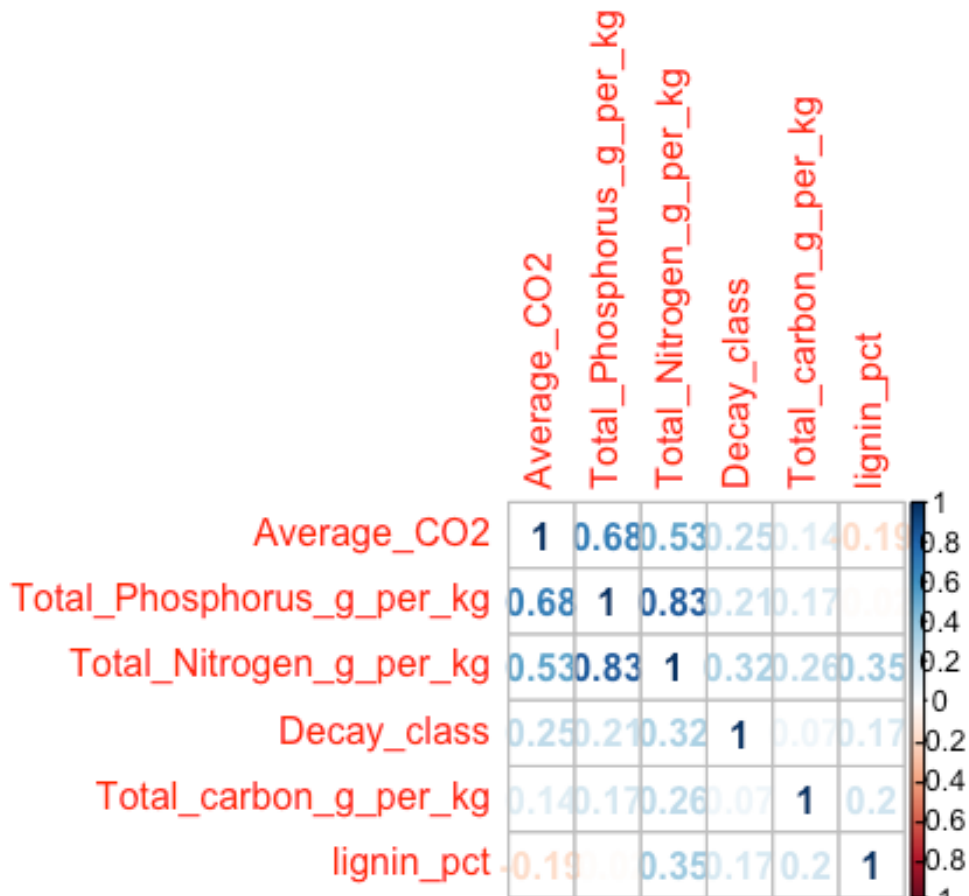
Total_Phosphorous_g/kg: Phosphorus as grams per dry kilogram of wood weight

lignin_%: Lignin as percent of dry wood-piece weight

Tag	Tree_species	Decay_class	Average_CO ₂	Total_carbon_g/kg	Total_Nitrogen_g/kg	Total_Phosphorus_g/kg	lignin_%
52	LC	1	0.529	458	3.96	0.20	26.8
160	LC	1	0.482	452	3.7	0.16	19.6
164	LC	1	0.335	455	3.51	0.12	19.7
2	LC	2	0.601	450	3.67	0.17	22.1
119	LC	2	1.980	496	4.30	0.22	18.6
214	LC	2	0.298	460	2.65	0.07	16.4
11	LC	3	0.450	458	3.08	0.13	23.7
67	LC	3	0.723	488	7.56	0.27	31.0
76	LC	3	0.404	491	4.69	0.11	25.2
92	LX	1	0.264	497	2.69	0.08	23.0
219	LX	1	0.358	454	3.33	0.20	19.3
223	LX	1	0.796	455	4.19	0.25	17.8
141	LX	2	1.146	492	5.78	0.36	16.0
142	LX	2	1.430	505	8.38	0.64	19.4
243	LX	2	0.392	454	3.44	0.11	24.8
191	LX	3	1.493	452	5.42	0.57	17.3
267	LX	3	1.454	459	7.40	0.37	24.0
269	LX	3	0.534	464	5.47	0.27	18.7
29	SN	1	0.269	455	2.29	0.06	16.7
40	SN	1	0.752	451	3.92	0.17	20.8
317	SN	1	0.463	527	2.42	0.12	20.6
7	SN	2	0.803	454	3.17	0.13	19.3
108	SN	2	0.980	453	1.45	0.07	16.2
313	SN	2	0.421	453	3.11	0.09	18.4
23	SN	3	0.449	470	3.19	0.14	19.2
25	SN	3	0.848	452	1.88	0.07	16.6
321	SN	3	0.335	503	3.13	0.10	21.8

Wood Chemistry: Supplementary Information S2

```
## [1] "Tag" "Tree_species"
## [3] "Decay_class" "Average_CO2"
## [5] "Total_carbon_g_per_kg" "Total_Nitrogen_g_per_kg"
## [7] "Total_Phosphorus_g_per_kg" "lignin_pct"
```



The high correlation between Total_Phosphorous_g_per_kg and Total_Nitrogen_g_per_kg means that we cannot include them in the same model (collinearity). So we run two separate models. We also run models separately for each decay class, because wood chemistry changes with age, due to selective retention of N and P while C is lost. This gives us 6 total models (3 decay classes X 2 models). As a result, we informally carry out a Table-wide correction of P-values by multiplying all P-values by 6 before assessing statistical significance.

Decay class 1

```
wood_dkc1 <- wood %>% filter(Decay_class == 1)

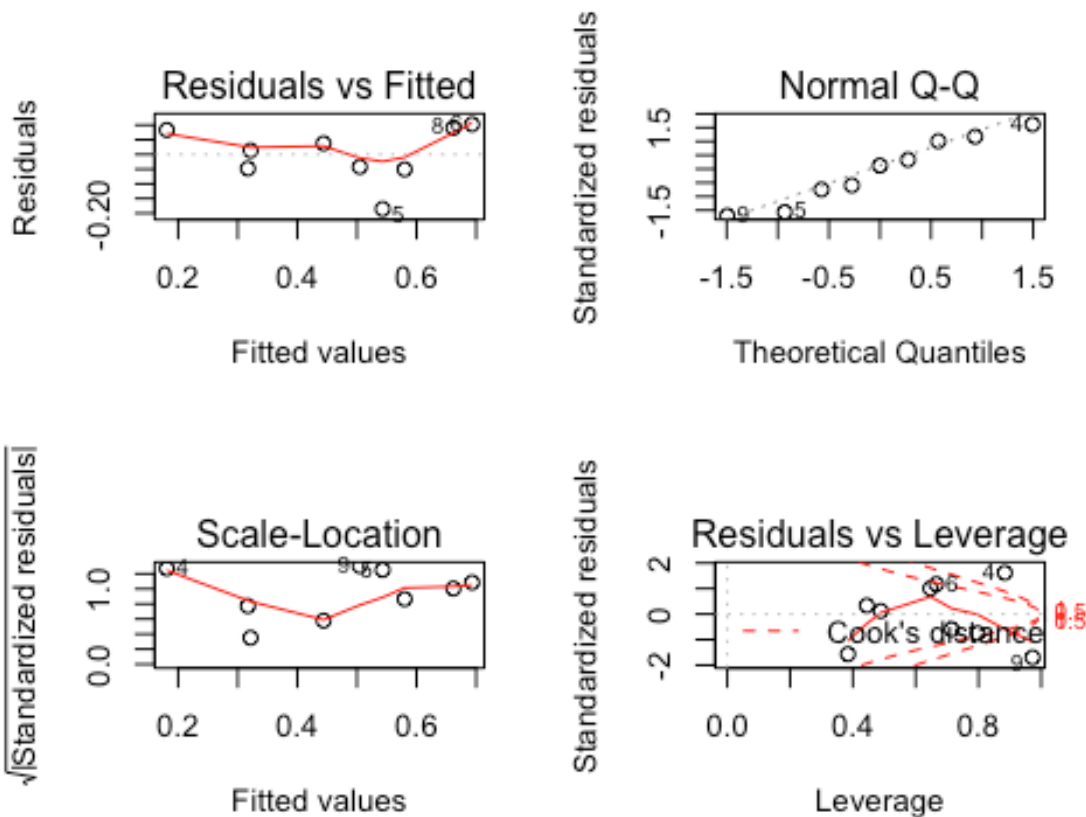
mod1.1 <- lm(Average_CO2 ~ Tree_species + Total_carbon_g_per_kg + Total_Phosphorus_g_per_kg + lignin_pct, data=wood_dkc1)
summary(mod1.1)

##
## Call:
## lm(formula = Average_CO2 ~ Tree_species + Total_carbon_g_per_kg +
##     Total_Phosphorus_g_per_kg + lignin_pct, data = wood_dkc1)
##
## Residuals:
##      1      2      3      4      5      6      7      8
## -0.05078  0.03754  0.01324  0.08299 -0.18550  0.10251 -0.04800  0.09029
##      9
## -0.04229
##
## Coefficients:
##              Estimate Std. Error t value Pr(>|t|)
## (Intercept)   -6.173e-02  1.132e+00  -0.055   0.9599
## Tree_speciesLX -2.262e-02  1.454e-01  -0.156   0.8863
## Tree_speciesSN  1.849e-01  1.553e-01   1.190   0.3195
## Total_carbon_g_per_kg -4.838e-05  2.635e-03  -0.018   0.9865
## Total_Phosphorus_g_per_kg  3.061e+00  1.061e+00   2.884   0.0633 .
## lignin_pct      1.936e-03  2.238e-02   0.087   0.9365
## ---
## Signif. codes:  0 '***' 0.001 '**' 0.01 '*' 0.05 '.' 0.1 ' ' 1
##
## Residual standard error: 0.1508 on 3 degrees of freedom
## Multiple R-squared:  0.775, Adjusted R-squared:  0.3999
## F-statistic: 2.066 on 5 and 3 DF,  p-value: 0.2921

vif(mod1.1)

##              GVIF Df GVIF^(1/(2*Df))
## Tree_species    1.929908  2      1.178648
## Total_carbon_g_per_kg  1.729095  1      1.314950
## Total_Phosphorus_g_per_kg  1.499699  1      1.224622
## lignin_pct      1.548025  1      1.244196

par(mfrow=c(2,2))
plot(mod1.1)
```



```
par(mfrow=c(1,1))
```

```
mod1.2 <- lm(Average_CO2 ~ Tree_species + Total_carbon_g_per_kg + Total_Nitro
gen_g_per_kg + lignin_pct, data=wood_dkc1)
summary(mod1.2)
```

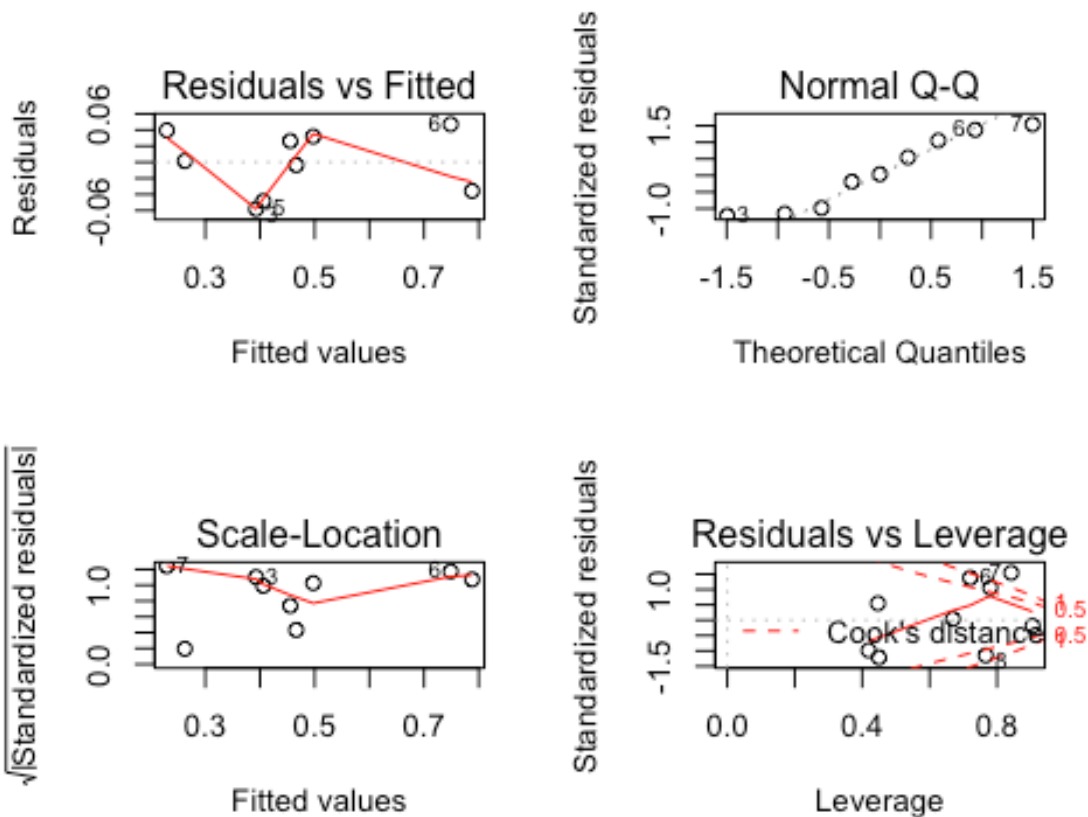
```
##
## Call:
## lm(formula = Average_CO2 ~ Tree_species + Total_carbon_g_per_kg +
##     Total_Nitrogen_g_per_kg + lignin_pct, data = wood_dkc1)
##
## Residuals:
##      1      2      3      4      5      6      7
## 0.031887 0.026213 -0.058099 0.001404 -0.048399 0.046995 0.039522
##      8      9
## -0.035806 -0.003717
##
## Coefficients:
```

```
##               Estimate Std. Error t value Pr(>|t|)
## (Intercept)    -2.171285   0.642439  -3.380   0.0431 *
## Tree_speciesLX    0.080254   0.059500   1.349   0.2702
## Tree_speciesSN    0.265343   0.067685   3.920   0.0295 *
## Total_carbon_g_per_kg  0.003182   0.001322   2.407   0.0953 .
## Total_Nitrogen_g_per_kg 0.376884   0.049140   7.670   0.0046 **
## lignin_pct      -0.010503   0.009978  -1.053   0.3698
## ---
## Signif. codes:  0 '***' 0.001 '**' 0.01 '*' 0.05 '.' 0.1 ' ' 1
##
## Residual standard error: 0.06452 on 3 degrees of freedom
## Multiple R-squared:  0.9588, Adjusted R-squared:  0.8901
## F-statistic: 13.96 on 5 and 3 DF, p-value: 0.02735

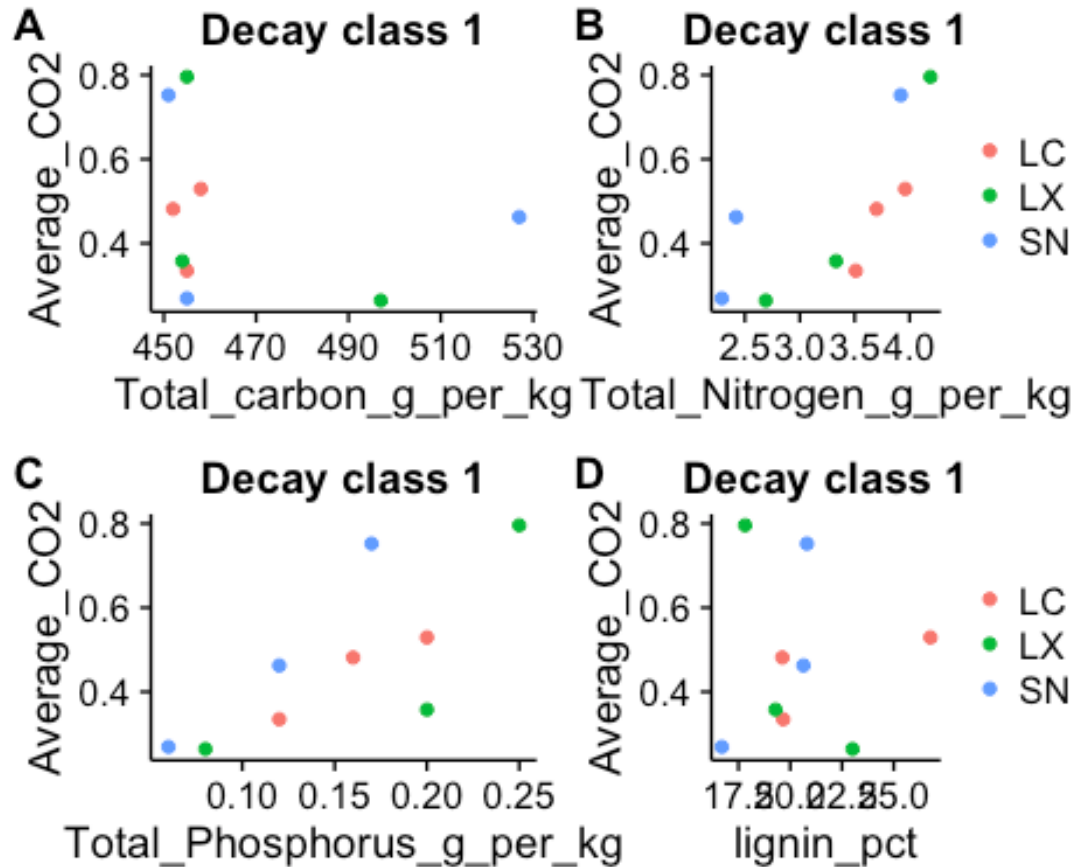
vif(mod1.2)

##               GVIF Df GVIF^(1/(2*Df))
## Tree_species    1.760129  2      1.151824
## Total_carbon_g_per_kg 2.376907  1      1.541722
## Total_Nitrogen_g_per_kg 2.304348  1      1.518008
## lignin_pct      1.680777  1      1.296448

par(mfrow=c(2,2))
plot(mod1.2)
```



```
par(mfrow=c(1,1))
```



Decay class 2

```
wood_dkc2 <- wood %>% filter(Decay_class == 2)
```

```
mod2.1 <- lm(Average_CO2 ~ Tree_species + Total_carbon_g_per_kg + Total_Phosphorus_g_per_kg + lignin_pct, data=wood_dkc2)
```

```
summary(mod2.1)
```

```
##
```

```
## Call:
```

```
## lm(formula = Average_CO2 ~ Tree_species + Total_carbon_g_per_kg +  
##     Total_Phosphorus_g_per_kg + lignin_pct, data = wood_dkc2)
```

```
##
```

```
## Residuals:
```

```
##      1      2      3      4      5      6      7  
## 0.174691 0.068453 -0.243143 0.089657 -0.080636 -0.009021 -0.011913  
##      8      9  
## 0.346874 -0.334961
```

```
##
```

```
## Coefficients:
```

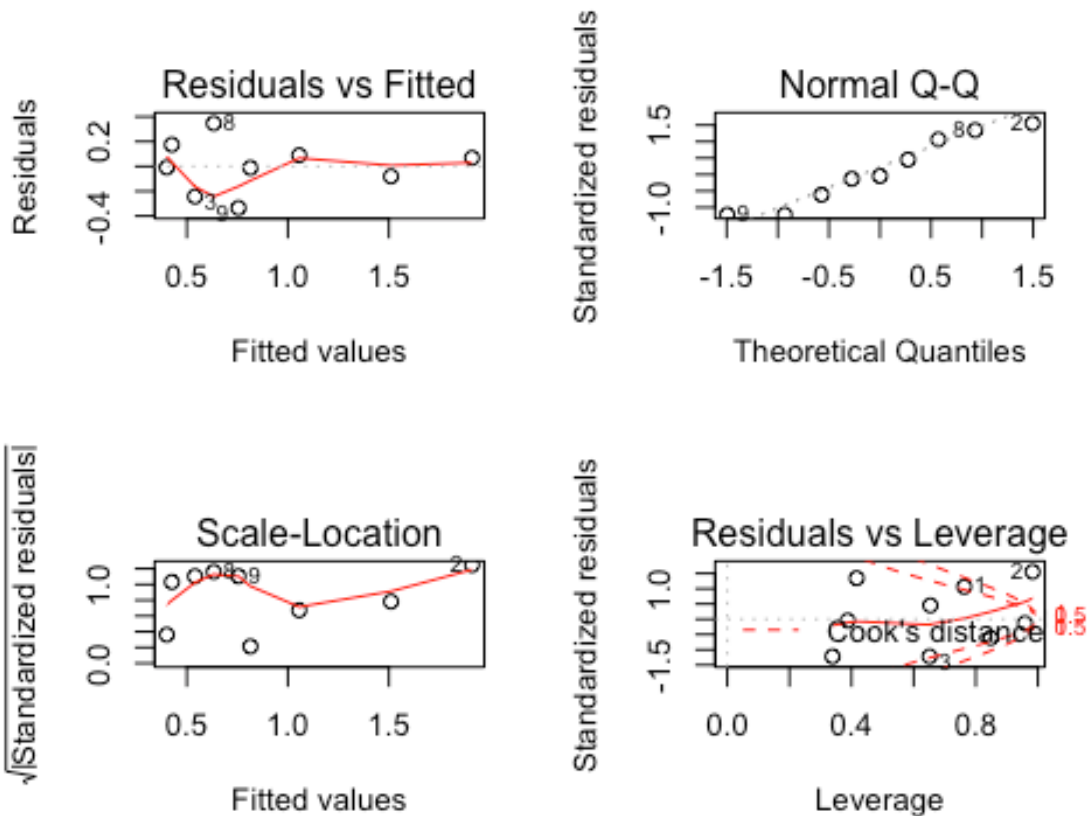
```
##              Estimate Std. Error t value Pr(>|t|)  
## (Intercept)   -18.00200     6.55221   -2.747   0.0709 .
```

```
## Tree_speciesLX          -0.40482    0.35162   -1.151    0.3330
## Tree_speciesSN          0.37527    0.33322    1.126    0.3420
## Total_carbon_g_per_kg    0.03817    0.01294    2.949    0.0601 .
## Total_Phosphorus_g_per_kg -0.93261    1.43524   -0.650    0.5621
## lignin_pct              0.06381    0.05536    1.153    0.3325
## ---
## Signif. codes:  0 '***' 0.001 '**' 0.01 '*' 0.05 '.' 0.1 ' ' 1
##
## Residual standard error: 0.3374 on 3 degrees of freedom
## Multiple R-squared:  0.8613, Adjusted R-squared:  0.6301
## F-statistic: 3.726 on 5 and 3 DF,  p-value: 0.154

vif(mod2.1)

##              GVIF Df GVIF^(1/(2*Df))
## Tree_species    3.044532  2      1.320931
## Total_carbon_g_per_kg  5.819261  1      2.412314
## Total_Phosphorus_g_per_kg  5.047178  1      2.246592
## lignin_pct       1.809937  1      1.345339

par(mfrow=c(2,2))
plot(mod2.1)
```



```

par(mfrow=c(1,1))

mod2.2 <- lm(Average_CO2 ~ Tree_species + Total_carbon_g_per_kg + Total_Nitro
gen_g_per_kg + lignin_pct, data=wood_dkc2)
summary(mod2.2)

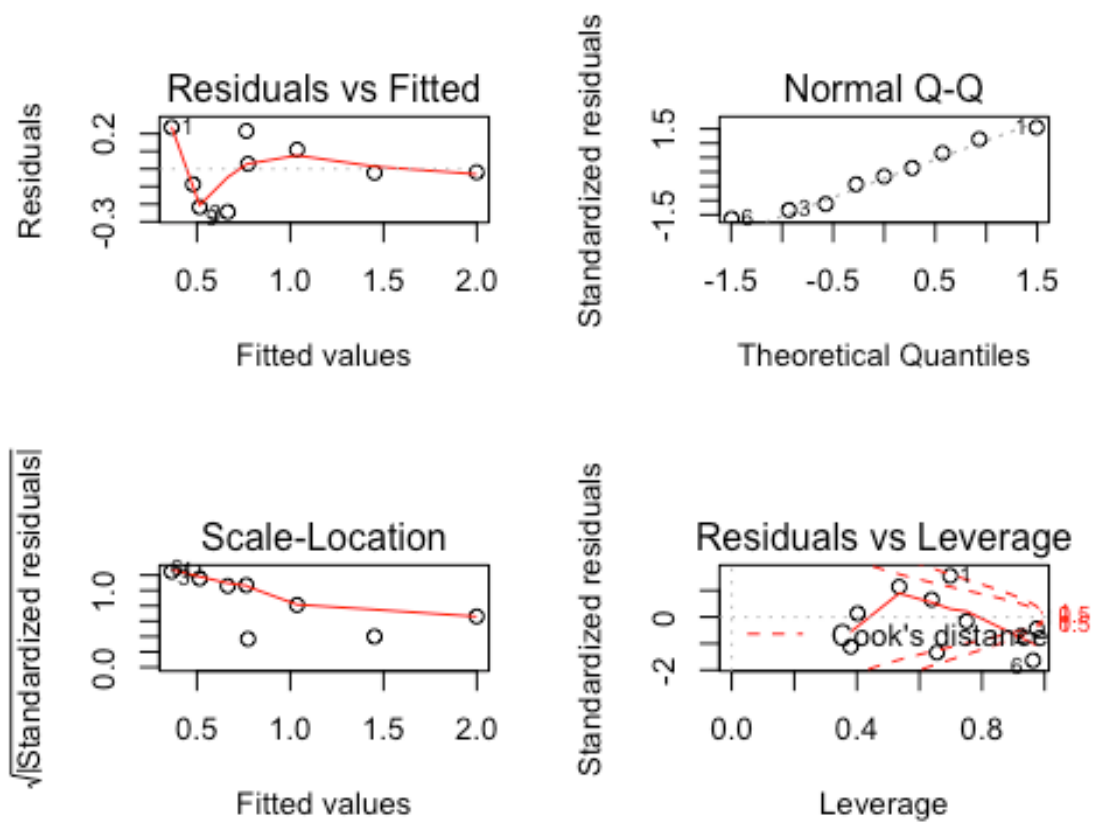
##
## Call:
## lm(formula = Average_CO2 ~ Tree_species + Total_carbon_g_per_kg +
##     Total_Nitrogen_g_per_kg + lignin_pct, data = wood_dkc2)
##
## Residuals:
##      1      2      3      4      5      6      7      8
## 0.23634 -0.01925 -0.21709  0.10930 -0.02207 -0.08722  0.02891  0.21552
##      9
## -0.24442
##
## Coefficients:
##              Estimate Std. Error t value Pr(>|t|)
## (Intercept)   -20.67956     5.46283  -3.786   0.0323 *
## Tree_speciesLX   -0.32065     0.29045  -1.104   0.3502
## Tree_speciesSN    0.37561     0.26721   1.406   0.2545
## Total_carbon_g_per_kg  0.04412     0.01097   4.022   0.0276 *
## Total_Nitrogen_g_per_kg -0.16922     0.11752  -1.440   0.2455
## lignin_pct      0.08208     0.04792   1.713   0.1853
## ---
## Signif. codes:  0 '***' 0.001 '**' 0.01 '*' 0.05 '.' 0.1 ' ' 1
##
## Residual standard error: 0.2771 on 3 degrees of freedom
## Multiple R-squared:  0.9064, Adjusted R-squared:  0.7505
## F-statistic: 5.813 on 5 and 3 DF,  p-value: 0.08912

vif(mod2.2)

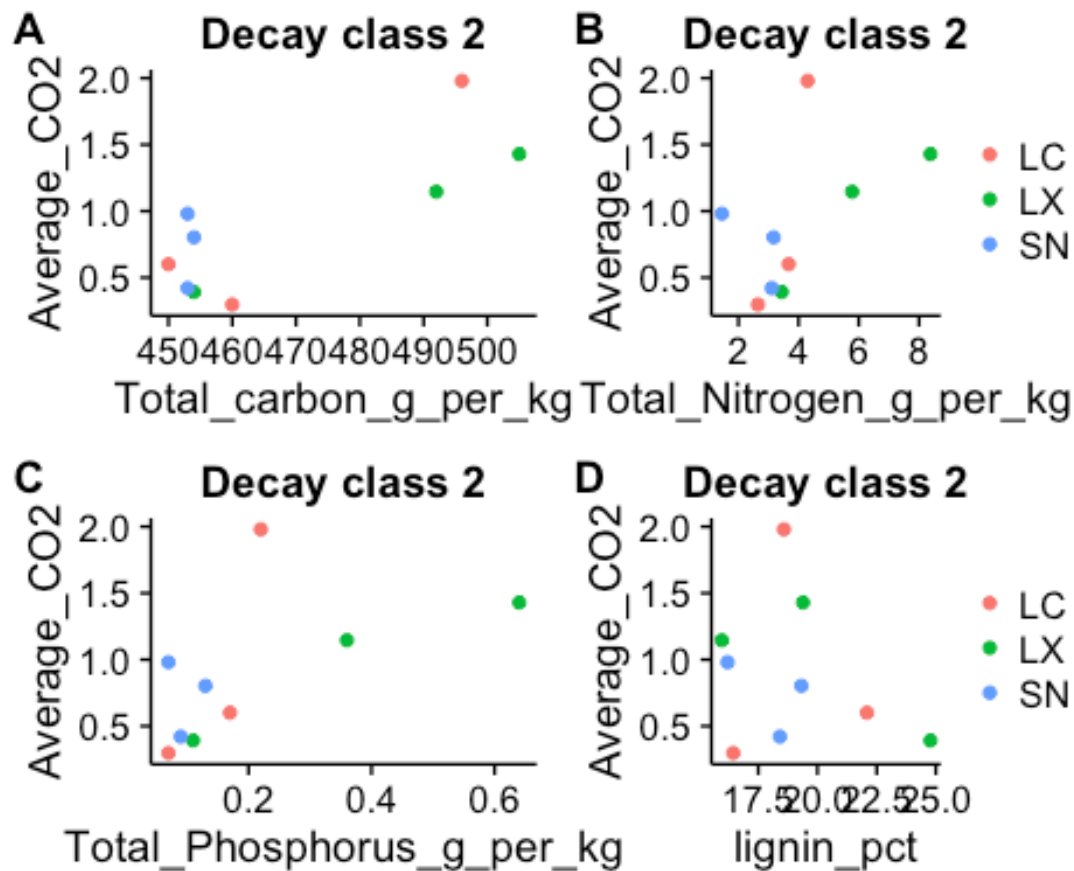
##              GVIF Df GVIF^(1/(2*Df))
## Tree_species      2.984744  2      1.314398
## Total_carbon_g_per_kg 6.196153  1      2.489207
## Total_Nitrogen_g_per_kg 5.874488  1      2.423734
## lignin_pct        2.010507  1      1.417923

par(mfrow=c(2,2))
plot(mod2.2)

```



```
par(mfrow=c(1,1))
```

Decay class 3

```
wood_dkc3 <- wood %>% filter(Decay_class == 3)
```

```
mod3.1 <- lm(Average_CO2 ~ Tree_species + Total_carbon_g_per_kg + Total_Phosphorus_g_per_kg + lignin_pct, data=wood_dkc3)
summary(mod3.1)
```

```
##
## Call:
## lm(formula = Average_CO2 ~ Tree_species + Total_carbon_g_per_kg +
##     Total_Phosphorus_g_per_kg + lignin_pct, data = wood_dkc3)
##
## Residuals:
##      1      2      3      4      5      6      7      8
## -0.12025 -0.09827  0.21852  0.05433  0.17236 -0.22669 -0.23209  0.20408
##      9
##  0.02801
##
## Coefficients:
##
##              Estimate Std. Error t value Pr(>|t|)
```

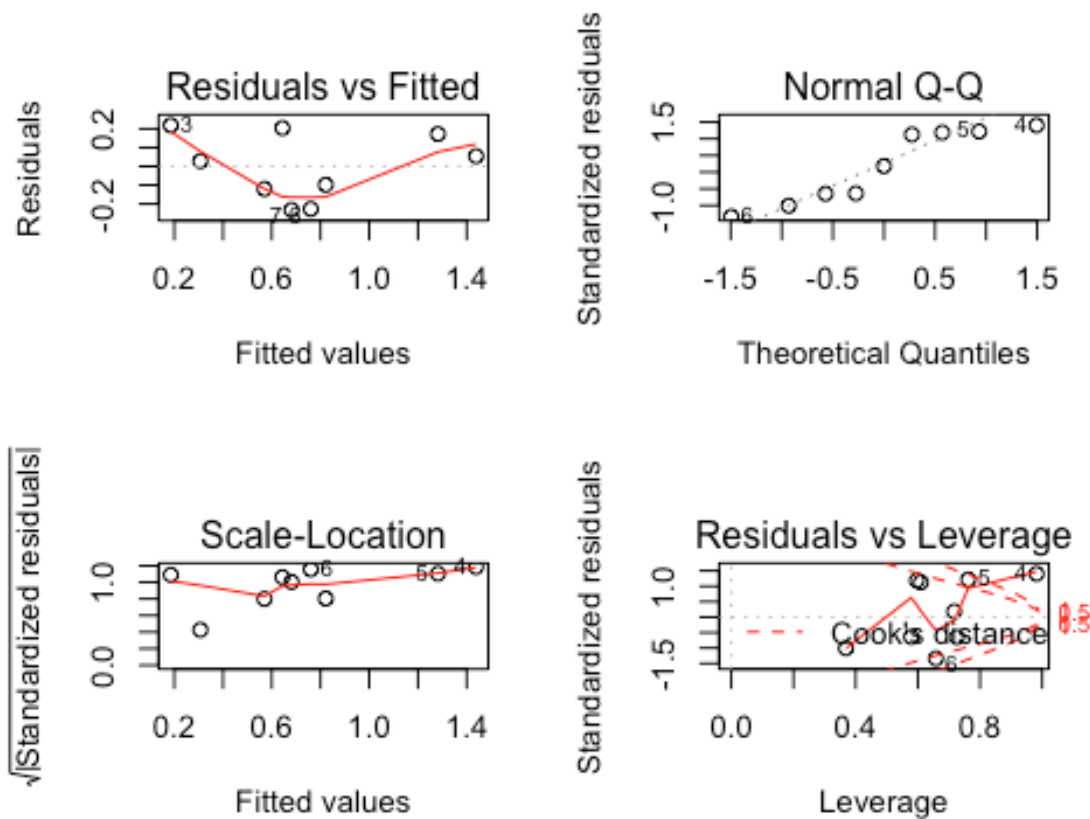
```
## (Intercept)          4.987860    3.305601    1.509    0.228
## Tree_speciesLX        0.231284    0.452830    0.511    0.645
## Tree_speciesSN        0.461017    0.389484    1.184    0.322
## Total_carbon_g_per_kg -0.012712    0.008088   -1.572    0.214
## Total_Phosphorus_g_per_kg 1.978470    1.168513    1.693    0.189
## lignin_pct            0.048483    0.044828    1.082    0.359
##
## Residual standard error: 0.29 on 3 degrees of freedom
## Multiple R-squared:  0.84, Adjusted R-squared:  0.5734
## F-statistic: 3.151 on 5 and 3 DF,  p-value: 0.1869
```

```
vif(mod3.1)
```

```
##              GVIF Df GVIF^(1/(2*Df))
## Tree_species 10.084610  2      1.782029
## Total_carbon_g_per_kg 2.176807  1      1.475401
## Total_Phosphorus_g_per_kg 3.462959  1      1.860903
## lignin_pct    4.046438  1      2.011576
```

```
par(mfrow=c(2,2))
```

```
plot(mod3.1)
```



```
par(mfrow=c(1,1))
```

```

mod3.1 <- lm(Average_CO2 ~ Tree_species + Total_carbon_g_per_kg + Total_Nitro
gen_g_per_kg + lignin_pct, data=wood_dkc3)
summary(mod3.1)

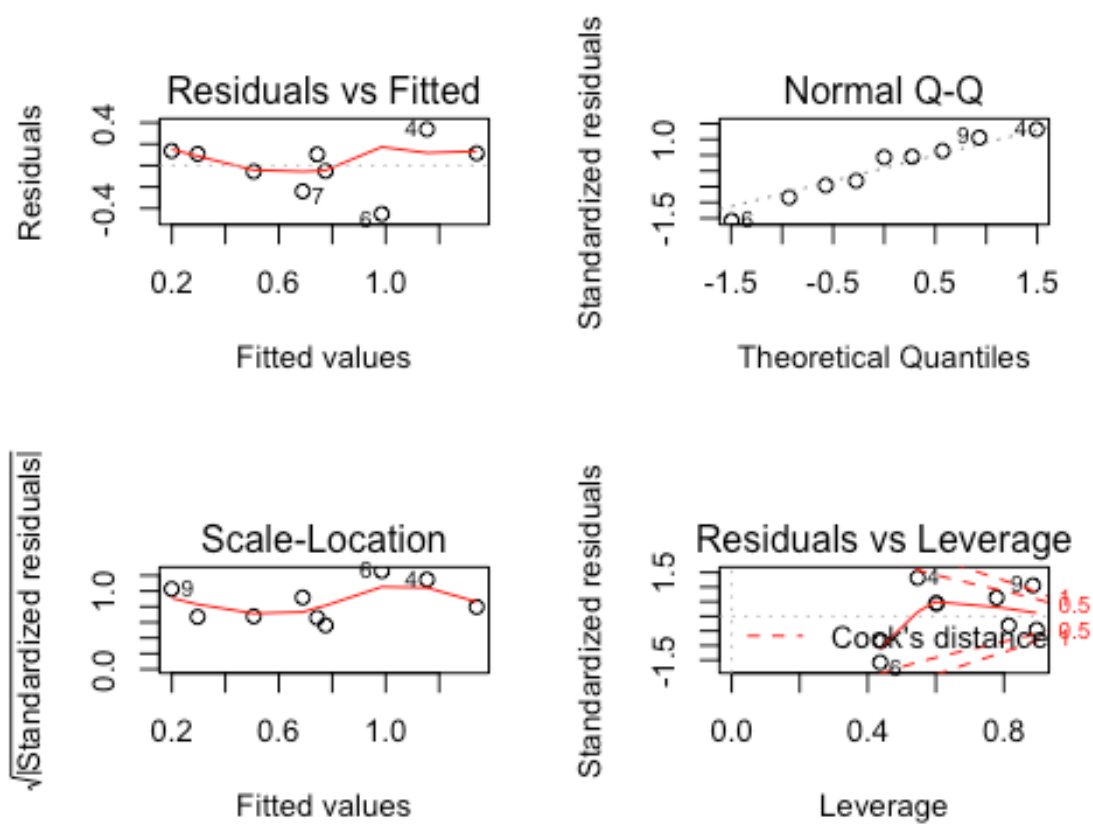
##
## Call:
## lm(formula = Average_CO2 ~ Tree_species + Total_carbon_g_per_kg +
##     Total_Nitrogen_g_per_kg + lignin_pct, data = wood_dkc3)
##
## Residuals:
##      1      2      3      4      5      6      7      8
## -0.05622 -0.05175  0.10797  0.33802  0.11382 -0.45185 -0.24040  0.10428
##      9
##  0.13612
##
## Coefficients:
##              Estimate Std. Error t value Pr(>|t|)
## (Intercept)      6.597447   4.439941   1.486   0.234
## Tree_speciesLX      0.140959   1.070537   0.132   0.904
## Tree_speciesSN      0.307366   0.552132   0.557   0.617
## Total_carbon_g_per_kg -0.014093   0.010568  -1.333   0.275
## Total_Nitrogen_g_per_kg  0.164312   0.262019   0.627   0.575
## lignin_pct      -0.006041   0.125806  -0.048   0.965
##
## Residual standard error: 0.3813 on 3 degrees of freedom
## Multiple R-squared:  0.7234, Adjusted R-squared:  0.2625
## F-statistic:  1.57 on 5 and 3 DF,  p-value: 0.3772

vif(mod3.1)

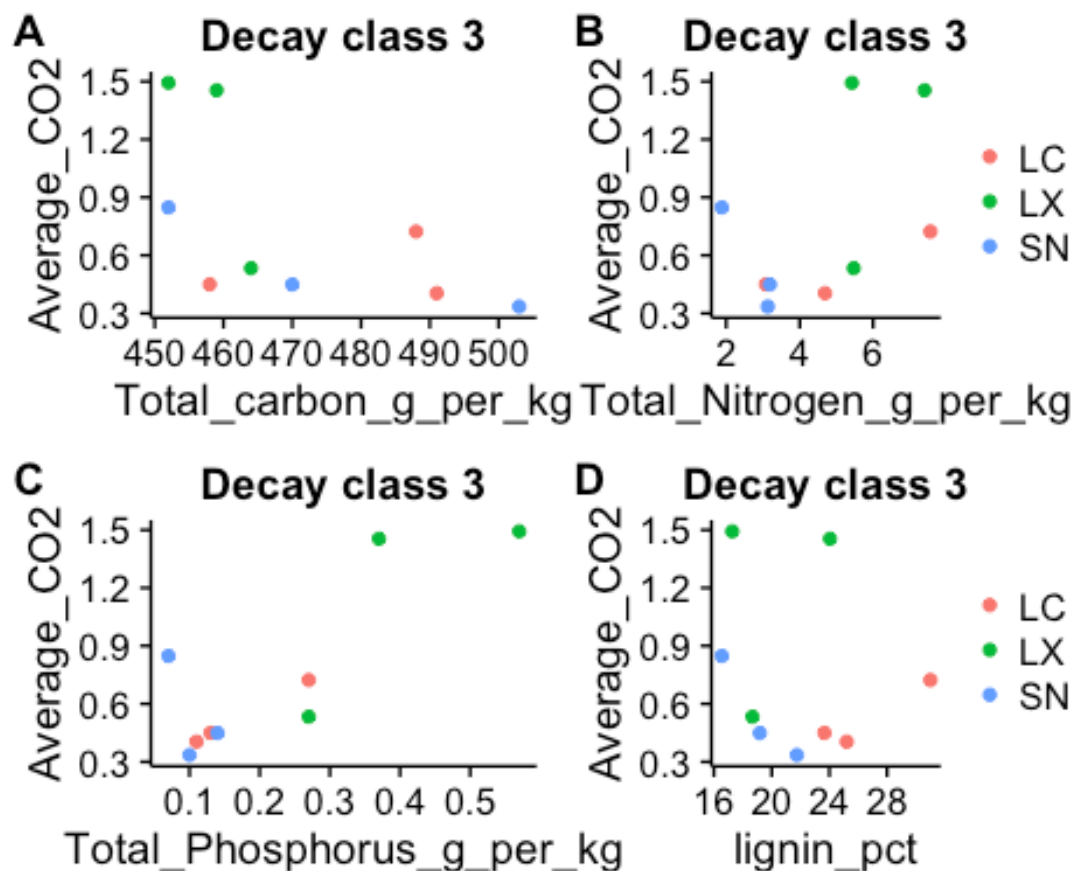
##              GVIF Df GVIF^(1/(2*Df))
## Tree_species      31.380994  2      2.366828
## Total_carbon_g_per_kg  2.149593  1      1.466149
## Total_Nitrogen_g_per_kg 15.056027  1      3.880210
## lignin_pct      18.432599  1      4.293320

par(mfrow=c(2,2))
plot(mod3.1)

```



```
par(mfrow=c(1,1))
```



```
sessionInfo()

## R version 3.3.0 (2016-05-03)
## Platform: x86_64-apple-darwin13.4.0 (64-bit)
## Running under: OS X 10.11.5 (El Capitan)
##
## locale:
## [1] en_GB.UTF-8/en_GB.UTF-8/en_GB.UTF-8/C/en_GB.UTF-8/en_GB.UTF-8
##
## attached base packages:
## [1] stats      graphics  grDevices utils      datasets  methods   base
##
## other attached packages:
## [1] car_2.1-2      corrplot_0.77 cowplot_0.6.2  ggplot2_2.1.0
## [5] dplyr_0.4.3    xlsx_0.5.7     xlsxjars_0.6.1 rJava_0.9-8
##
## loaded via a namespace (and not attached):
## [1] Rcpp_0.12.5      formatR_1.4      nloptr_1.0.4
## [4] plyr_1.8.4       tools_3.3.0      digest_0.6.9
## [7] lme4_1.1-12      evaluate_0.9      gtable_0.2.0
```

```
## [10] nlme_3.1-128      lattice_0.20-33    mgcv_1.8-12
## [13] Matrix_1.2-6      DBI_0.4-1          yaml_2.1.13
## [16] parallel_3.3.0    SparseM_1.7        stringr_1.0.0
## [19] knitr_1.13        MatrixModels_0.4-1 grid_3.3.0
## [22] nnet_7.3-12       R6_2.1.2           rmarkdown_0.9.6
## [25] minqa_1.2.4       magrittr_1.5       scales_0.4.0
## [28] htmltools_0.3.5   MASS_7.3-45        splines_3.3.0
## [31] assertthat_0.1    pbkrtest_0.4-6     colorspace_1.2-6
## [34] labeling_0.3      quantreg_5.26      stringi_1.1.1
## [37] lazyeval_0.1.10   munsell_0.4.3
```

Higher fungal diversity is correlated with lower CO₂ emissions from dead wood in a natural forest:

S3 Sandau et al. analyses

fungus_Sandau_analysis.R

Negorashi2011

Thu Oct 30 17:34:54 2014

```
#####  
bioRxiv preprint doi: https://doi.org/10.1101/051233; this version posted June 13, 2016. The copyright holder for this preprint (which was  
not certified by peer review) is the author/funder. All rights reserved. No reuse allowed without permission.  
### R routine to include correlation structure in a linear model.  
### (modified from Sandau et al 2014 in MEE by Viorel D. Popescu)  
#####  
## MAIN FUNCTIONS  
#####  
# FOR ALL FUNCTIONS THE INPUT PARAMETERS ARE:  
# y = RESPONSE VARIABLE  
# x = DESIGN MATRIX OF EXPLANATORY VARIABLES  
# zf = DESIGN MATRIX FOR THE FIRST RANDOM EFFECT  
# zt = DESIGN MATRIX FOR THE SECOND RANDOM EFFECT  
# M = CORRELATION MATRIX  
  
# THE OUTPUT IS A LIST CONTAINING:  
# beta = MAXIMUM LIKELIHOOD ( OR RESTRICTED MAXIMUM LIKELIHOOD ) ESTIMATION OF THE FIXED  
PARAMETERS  
# se = STANDARD ERRORS OF THE FIXED PARAMETERS  
# T = T-VALUES OF THE FIXED PARAMETERS  
# pvalue = P-VALUE OF THE FIXED PARAMETERS  
# lambda = LAMBDA PARAMETER FOR THE STRENGTH OF THE CORRELATION STRUCTURE  
# sigma2 = OVERALL VARIANCE OF THE RESIDUALS  
# loglike = MAXIMUM LOG-LIKELIHOOD ESTIMATION ( OR RESTRICTED LOG-LIKELIHOOD )  
  
rm(list=ls())  
  
# Run these functions once before all the Sandau et al. analyses #  
#### START FUNCTIONS for MODEL W/CORRELATION STRUCTURE m_corr MODEL #####  
#####  
#MAXIMUM LIKELIHOOD ESTIMATOR WITH CORRELATION STRUCTURE  
  
fit_ML <- function(y,X,M){  
  
  n <- length(y)  
  p <- dim(X)[2]  
  f <- function(a){-profile_ML_psi_lambda(1/(1+exp(-a[1])),y,X,M)}  
  out <- optim(c(0), f, method="SANN")  
  print(out)  
  lambda <- 1 / (1 + exp(-out$par[1]))  
  M2 <- M * lambda + diag(diag(M)) * (1-lambda)  
  Pi <- solve(M2)  
  out2 <- ML_beta_sigma(y,X,Pi)
```



```

T <- out2$beta / out2$se
pvalue <- dt(T,n-p)
loglike <- -0.5 * n * log(2*pi) -1/(2*out2$sigma2) * t(y - X %*% out2$beta) %*% Pi %*
% (y - X %*% out2$beta) -0.5 * n * log(out2$sigma2) + 0.5 * determinant(Pi,logarithm=TRUE)
E)$modulus[1]
out3 <- c(out2, list(T = T, pvalue = pvalue, lambda = lambda, loglike = as.vector(logl
ike)))

```

bioRxiv preprint doi: <https://doi.org/10.1101/051235>; this version posted June 13, 2016. The copyright holder for this preprint (which was not certified by peer review) is the author/funder. All rights reserved. No reuse allowed without permission.

```

}

```

```

## profile function

```

```

ML_beta_sigma <- function(y,X,Pi){

```

```

  n <- dim(X)[1]
  p <- dim(X)[2]
  beta <- solve( (t(X) %*% Pi %*% X), t(X) %*% Pi %*% y)
  sigma2 <- 1/n * t(y - X %*% beta) %*% Pi %*% (y - X %*% beta)
  se <- sqrt( diag( solve(t(X) %*% Pi %*% X) ) * sigma2 )
  out <- list(beta = as.vector(beta), sigma2 = sigma2, se = se)
  out

```

```

}

```

```

###

```

```

profile_ML_psi_lambda <- function(lambda,y,X,M){

```

```

  n <- length(y)
  M2 <- M * lambda + diag(diag(M)) * (1-lambda)
  Pi <- solve(M2)
  out <- ML_beta_sigma(y,X,Pi)
  l <- -0.5 * n * log(out$sigma2) + 0.5 * determinant(Pi,logarithm=TRUE)$modulus[1]
  l

```

```

}

```

```

### END FUNCTIONS for MODEL W/CORRELATION STRUCTURE m_corr MODEL ###

```

```

### START FUNCTIONS for MODEL W/O CORRELATION STRUCTURE m_ref MODEL ####

```

```

fit_ML_without_lambda <- function(y,X){

```

```

  M <- diag(rep(1,length(y)))
  n <- length(y)
  p <- dim(X)[2]
  f <- function(a){-profile_ML_psi(y,X,M)}
  #out <- optim(c(0,0), f)

```

bioRxiv preprint doi: <https://doi.org/10.1101/051235>; this version posted June 13, 2016. The copyright holder for this preprint (which was not certified by peer review) is the author/funder. All rights reserved. No reuse allowed without permission.

```

Pi <- solve(M)
out2 <- ML_beta_sigma(y,X,Pi)
T <- out2$beta / out2$se
pvalue <- dt(T,n-p)
loglike <- -0.5 * n * log(2*pi) -1/(2*out2$sigma2) * t(y - X %%% out2$beta) %%% Pi %*
% (y - X %%% out2$beta) -0.5 * n * log(out2$sigma2) + 0.5 * determinant(Pi,logarithm=TRU
E)$modulus[1]
out3 <- c(out2, list(T=T, pvalue=pvalue, loglike=loglike, se=se))
out3

}

ML_beta_sigma <- function(y,X,Pi){

  n <- dim(X)[1]
  p <- dim(X)[2]
  beta <- solve( (t(X) %%% Pi %%% X), t(X) %%% Pi %%% y)
  sigma2 <- 1/n * t(y - X %%% beta) %%% Pi %%% (y - X %%% beta)
  se <- sqrt( diag( solve(t(X) %%% Pi %%% X) ) * sigma2 )
  out <- list(beta = as.vector(beta), sigma2 = sigma2, se = se)
  out

}

profile_ML_psi <- function(y,X,M){
  n <- length(y)
  Pi <- solve(M)
  out <- ML_beta_sigma(y,X,Pi)
  l <- -0.5 * n * log(out$sigma2) + 0.5 * determinant(Pi,logarithm=TRUE)$modulus[1]
  l
}

#### END FUNCTIONS for MODEL W/O CORRELATION STRUCTURE m_ref MODEL ####

#### START THE ANALYSES #####
library(vegan)

```

```

## Loading required package: permute
## Loading required package: lattice
## This is vegan 2.0-10

```

```
library(car)
```

```
setwd("~/Dropbox/Working Docs/Barcode soup censuses/Schaefer, Fungus/analyses 31 Oct 2014 Doug Viorel")
```

```
# June2012CO2.crop.lc.txt #
```

```
# June2012CO2.crop.lx.txt #
```

bioRxiv preprint doi: <https://doi.org/10.1101/057235>; this version posted June 13, 2016. The copyright holder for this preprint (which was not certified by peer review) is the author/funder. All rights reserved. No reuse allowed without permission.

```
# June2012CO2.crop.sn.txt, omitting influential woodpieceID=110 #
```

```
# June2013CO2.crop.lc.txt #
```

```
# June2013CO2.crop.lx.txt, omitting woodpieceID=95 because no CO2 value #
```

```
# June2013CO2.crop.sn.txt, omitting woodpieceID=31 because no CO2 value#
```

```
# June2012CO2.uclust.lc.txt #
```

```
# June2012CO2.uclust.lx.txt #
```

```
# June2012CO2.uclust.sn.txt, omitting influential woodpieceID=110 #
```

```
# June2013CO2.uclust.lc.txt #
```

```
# June2013CO2.uclust.lx.txt, omitting woodpieceID=95 because no CO2 value #
```

```
# June2013CO2.uclust.sn.txt, omitting woodpieceID=31 because no CO2 value#
```

```
filename <- 'June2012CO2.crop.lc.txt' # i paste each file name from the list above into  
this command, select all (which starts the run by clearing the workspace), and run all c  
ommands. Then repeat for each file
```

```
fung <- read.table(filename,header=TRUE)
```

```
colnames(fung)[2] <- "CO2"
```

```
names(fung[,1:2])
```

```
## [1] "Fungus.apn.lc.run1.sep.env.woodpieceID"
```

```
## [2] "CO2"
```

```
# str(fung)
```

```
nrow(fung) # because number of rows differs across months
```

```
## [1] 25
```

```
ncol(fung) # because number of cols differs between CROP and uclust
```

```
## [1] 2866
```

```

# calculate the similarity matrix (1 - Jaccard dissimilarity)
# rows and cols in the 'fung' matrix vary across dates and wood species
M.fung.dis <- as.dist(vegdist(fung[1:nrow(fung),3:ncol(fung)], binary=T, method="jaccard
"))
M.fung <- 1-as.matrix(M.fung.dis)

# Predicted variable is CO2 emissions
Y.fung.CO2 = as.matrix(fung$CO2)

# Predictor variable is the Shannon diversity index
# rows and cols in the 'fung' matrix vary across dates and wood species
X.fung.div = as.matrix(diversity(fung[1:nrow(fung),3:ncol(fung)]))

# Get the design matrix for the model [Y.fung.CO2 ~ X.fung.div]
X.fungi = as.matrix(model.matrix(Y.fung.CO2~X.fung.div))

## Fit LM MODEL ##

m_lm=lm(Y.fung.CO2~X.fung.div)
summary(m_lm)

```

```

##
## Call:
## lm(formula = Y.fung.CO2 ~ X.fung.div)
##
## Residuals:
##      Min       1Q   Median       3Q      Max
## -1.2371 -0.3129 -0.1149  0.2254  1.9306
##
## Coefficients:
##              Estimate Std. Error t value Pr(>|t|)
## (Intercept)    2.4957     0.4281   5.830 6.11e-06 ***
## X.fung.div     -0.5366     0.1814  -2.957  0.00706 **
## ---
## Signif. codes:  0 '***' 0.001 '**' 0.01 '*' 0.05 '.' 0.1 ' ' 1
##
## Residual standard error: 0.7508 on 23 degrees of freedom
## Multiple R-squared:  0.2755, Adjusted R-squared:  0.244
## F-statistic: 8.746 on 1 and 23 DF,  p-value: 0.007061

```

```
plot(X.fung.div, Y.fung.CO2)
abline(lm(Y.fung.CO2 ~ X.fung.div))
```

Fit Model WITH CORRELATION STRUCTURE

```
m_corr <- fit_ML(Y.fung.CO2, X.fungi, M.fungi)
```

bioRxiv preprint doi: <https://doi.org/10.1101/051285>; this version posted June 12, 2016. The copyright holder for this preprint (which was not certified by peer review) is the author/funder. All rights reserved. No reuse allowed without permission.

```
## $par
## [1] -17.52438
##
## $value
## [1] -8.209146
##
## $counts
## function gradient
##      10000      NA
##
## $convergence
## [1] 0
##
## $message
## NULL
```

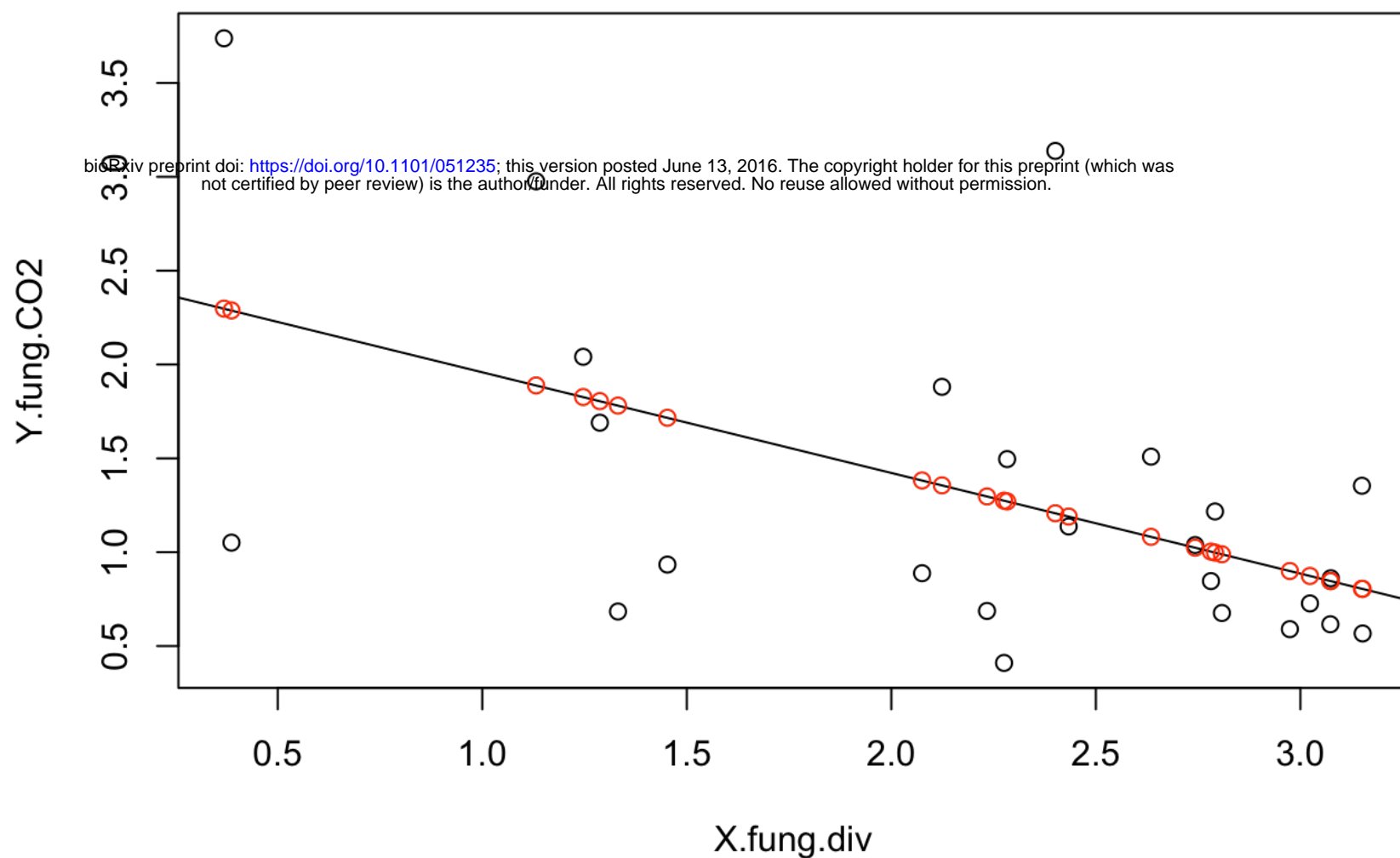
m_corr # look at the lambda value, which is the strength of the correlation structure. With input dataset JuneOTU.lc.txt, the lambda value is close to zero, meaning almost no effect of the community structure on the amount of CO2 released. Consequently, the coefficient estimates, p-values and loglikelihood are similar to the lm model.

```
## $beta
## [1] 2.4957317 -0.5366139
##
## $sigma2
## [1,] 0.5185433
##
## bioRxiv preprint doi: https://doi.org/10.1101/051235; this version posted June 13, 2016. The copyright holder for this preprint (which was
## $se not certified by peer review) is the author/funder. All rights reserved. No reuse allowed without permission.
## [1] 0.4106264 0.1740396
##
## $T
## [1] 6.077865 -3.083286
##
## $pvalue
## [1] 4.020548e-06 6.212384e-03
##
## $lambda
## [1] 2.450513e-08
##
## $loglike
## [1] -27.26432
```

```
predicted = m_corr$beta[1] + m_corr$beta[2]*X.fung.div
predicted; points(X.fung.div, predicted, col="red") # With the JuneOTU.lc.txt dataset, t
he
```

```
##          [,1]
## 1  0.8051847
## 2  0.8733322
## 3  2.2978963
## 4  1.2073624
## 5  0.8997118
## 6  0.8459969
## 7  1.8267251
## 8  1.2746412
## 9  1.7810741
## 10 1.0817882
## 11 1.7162385
## 12 1.3560805
## 13 0.9979075
## 14 2.2881198
## 15 1.8884770
## 16 1.3821675
## 17 1.0240120
## 18 0.9888807
## 19 1.0031981
## 20 0.8466022
## 21 1.2706007
## 22 0.8042258
## 23 1.1899057
## 24 1.2969998
## 25 1.8048714
```

bioRxiv preprint doi: <https://doi.org/10.1101/051235>; this version posted June 13, 2016. The copyright holder for this preprint (which was not certified by peer review) is the author/funder. All rights reserved. No reuse allowed without permission.



```
### END MODEL WITH CORRELATION STRUCTURE
```

```
### FIT REFERENCE MODEL (no correlation structure)
```

```
m_ref <- fit_ML_without_lambda(Y.fung.CO2,X.fungi)
```

```
m_ref
```



```
## $beta
## [1] 2.4957317 -0.5366139
##
## $sigma2
## [1,] 0.5185433
##
## bioRxiv preprint doi: https://doi.org/10.1101/051235; this version posted June 13, 2016. The copyright holder for this preprint (which was
## $se not certified by peer review) is the author/funder. All rights reserved. No reuse allowed without permission.
## [1] 0.4106264 0.1740396
##
## $T
## [1] 6.077865 -3.083286
##
## $pvalue
## [1] 4.020548e-06 6.212384e-03
##
## $loglike
## [1] -27.26432
```

```
### END REFERENCE MODEL
```

```
# estimation of p-value of lambda (see Zuur et al. 2009, pp. 123-124)
pl <- 0.5*(1-pchisq(m_corr$loglike-m_ref$loglike,1))
pl
```

```
## [1] 0.5
```

```
# write results to a table
results <- cbind(filename,m_corr$lambda,pl)
write.table(results,"Sandau et al results.txt",append = TRUE,sep="\t",col.names=FALSE,qu
ote=FALSE)
```

Higher fungal diversity is correlated with lower CO₂ emissions from dead wood in a natural forest:

S4 Conventional Community Analyses

Supporting Information S4. Conventional community analyses to test for an effect of fungal community composition *per se* on CO₂ emissions.

Methods

We removed singleton OTUs (OTUs occurring in only one sample) and visualized the OTU tables using correspondence analysis (*cca()* in *R*). We tested the hypothesis that CO₂ emissions explain variation in community composition by using: (1) *cca*(OTUtable ~ CO₂) + *anova*(by="term", perm=9999) in *vegan* (**Oksanen et al., 2013**) and (2) *manyglm*(OTUtable ~ CO₂, family="negative binomial") + *anova*(resamp="pit.trap", nBoot=999) in *mvabund* (**Warton et al., 2012**). As four versions of each OTU table were tested, we Bonferroni-corrected for multiple tests by multiplying the resulting p-values by 4. *mvabund* is a multivariate implementation of generalized linear models, and unlike dissimilarity-based methods such as *cca*, *mvabund* does not confound location with dispersion effects, which can inflate both type 1 and 2 errors (**Warton et al., 2012**). Based on the correspondence-analysis plots, we deemed some low-diversity wood pieces to be possible influential outliers (*i.e.* individual samples likely to be largely responsible for any significant community effects), and we removed these data points and repeated the analyses.

Results

After Bonferroni correction, no June 2012 samples showed significant effects of fungal composition on CO₂ emissions, regardless of wood species, statistic, OTU-clustering method, or rarefaction (Table S4).

For June 2013 samples, CCA detected marginally significant effects of composition for all three wood species after Bonferroni correction, but for LC and LX, statistical significance relied on one or two highly dissimilar, low-fungal-diversity wood samples (Main text, Fig. 2). For SN, significant CCA effects were robust to the removal of three potentially influential points, but the *mvabund* test for SN was non-significant after Bonferroni correction. Overall, our data do not reject the null hypothesis that higher fungal species diversity *per se*, and not any particular fungal species, is responsible for reducing CO₂ emissions.

References

- Oksanen J, Blanchet FG, Kindt R, Legendre P, Minchin RB, O'Hara RB, et al. 2013. *vegan*: Community Ecology R package version 2.0-10. Available at: <http://CRAN.R-project.org/package=vegan>. Last accessed 30 May 2014.
- Warton DI, Wright ST, Wang Y. 2012. Distance-based multivariate analyses confound location and dispersion effects. *Meth Ecol Evol* **3**:89-101. doi:10.1111/j.2041-210X.2011.00127.x.

Table S4. Inferring a ‘pure diversity’ effect of fungal communities on CO₂ emissions. For each of the six fungal communities visualized in Figure 2, two statistical methods (canonical correspondence analysis and *mvabund*, see Methods), were used to test for significant effects of fungal community composition on CO₂ emissions. For all June 2012 CO₂ samples, no significant effects of fungal community (September 2012) were found. For the June 2013 CO₂ samples, marginally significant effects after Bonferroni correction ($p < 0.05$) were detected, but only by CCA, not by *mvabund*. Moreover, the significant CCA effects in the two *Lithocarpus* species were not robust to the removal of a few outlying, low-diversity wood pieces, as seen in Fig. 2. Wood species are indicated by LC, LX, SN, for *Lithocarpus chintungensis*, *L. xylocarpus*, and *Schima noronhae*, respectively.

CO ₂ sample date ¹	Species	Test method	Low-diversity wood pieces removed? ²	p-value range ³
June 2012	LC	CCA	no, full dataset	0.10-0.37
			14 removed	0.13-0.39
		<i>mvabund</i>	no, full dataset	0.15-0.23
	LX	CCA	no, full dataset	0.04-0.09
			9, 15 removed	0.17-0.26
		<i>mvabund</i>	no, full dataset	0.39-0.47
June 2013	SN	CCA	no, full dataset	0.09-0.15
			7, 10 removed	0.04-0.24
		<i>mvabund</i>	no, full dataset	0.06-0.54
	LC	CCA	no, full dataset	0.01-0.02*
			9, 17 removed	0.17-0.46
		<i>mvabund</i>	no, full dataset	0.03-0.08
June 2013	LX	CCA	no, full dataset	0.01-0.03*
			9 removed	0.04-0.18
		<i>mvabund</i>	no, full dataset	0.15-0.32
	SN	CCA	no, full dataset	0.01-0.02*
			10, 11, 14 removed	0.01-0.05*
		<i>mvabund</i>	no, full dataset	0.03-0.05

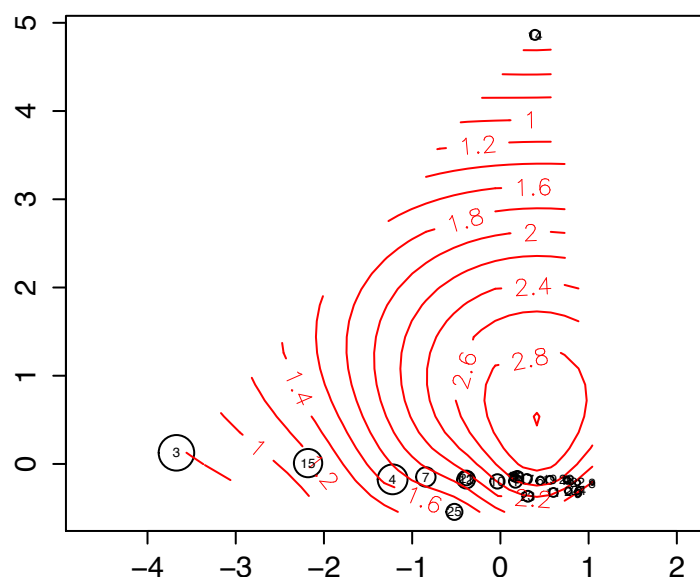
¹ September 2012 fungal community was tested against June 2012 CO₂ emissions, as in Fig. 1.

² Numbers refer to points in Fig. 2.

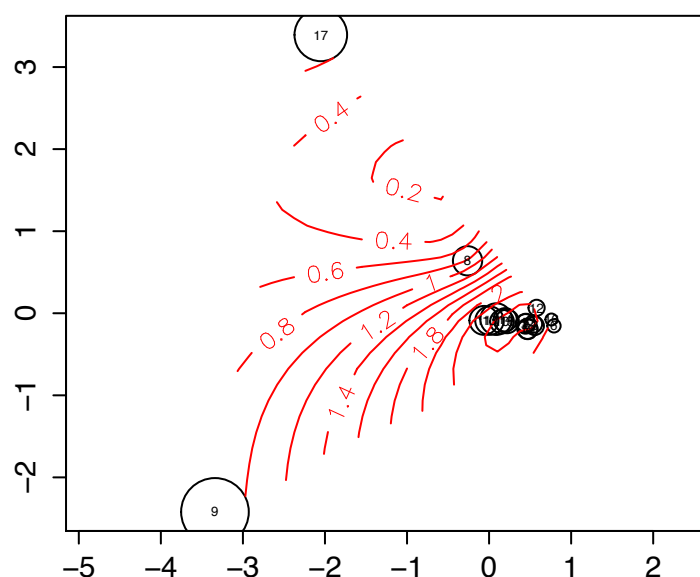
³ Asterisks indicate formally significant effects ($p < 0.05$) after Bonferroni correction for four tests: CROP/non-rarefied, CROP/rarefied, *uclust*/non-rarefied, and *uclust*/rarefied. Original p-values reported here.

bioRxiv preprint doi: <https://doi.org/10.1101/051235>; this version posted June 13, 2016. The copyright holder for this preprint (which was not certified by peer review) is the author/funder. All rights reserved. No reuse allowed without permission.

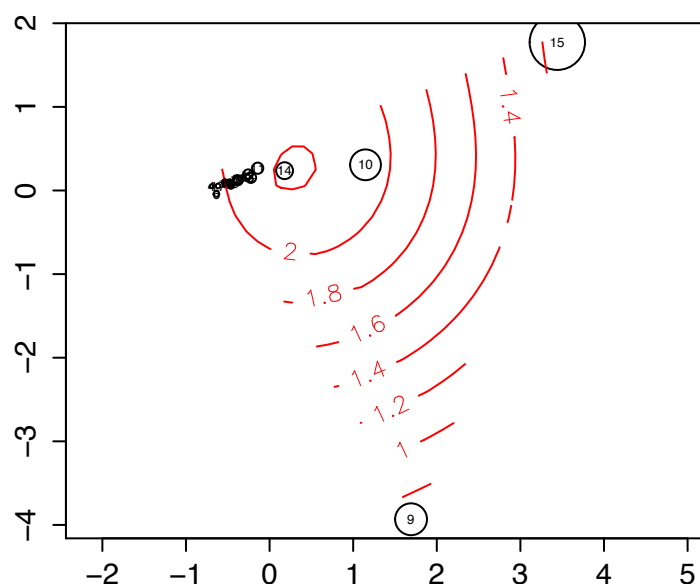
LC, June 2012 CO₂ ~ Sep 2012 Shannon



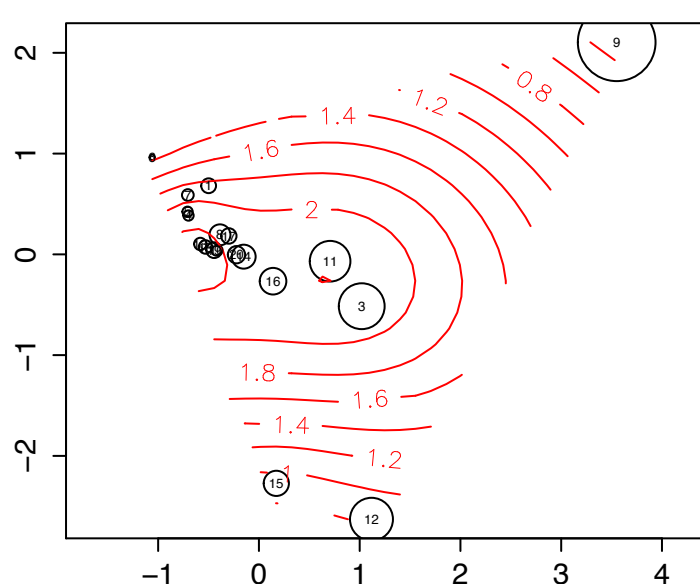
LC, June 2013 CO₂ ~ June 2013 Shannon



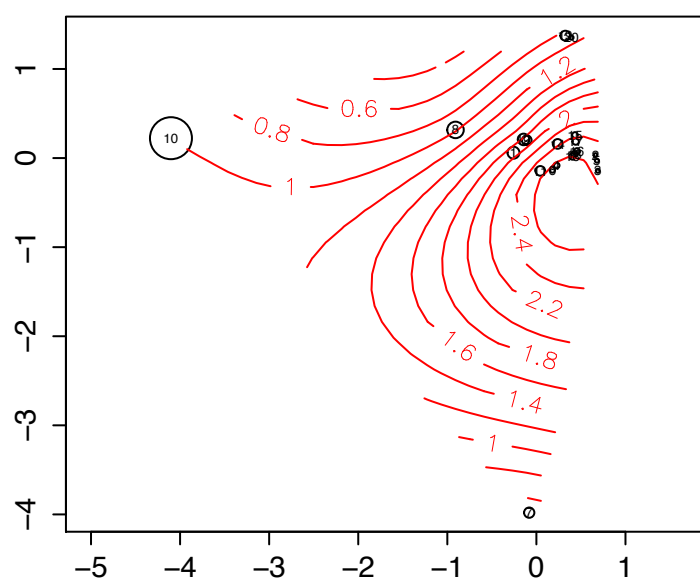
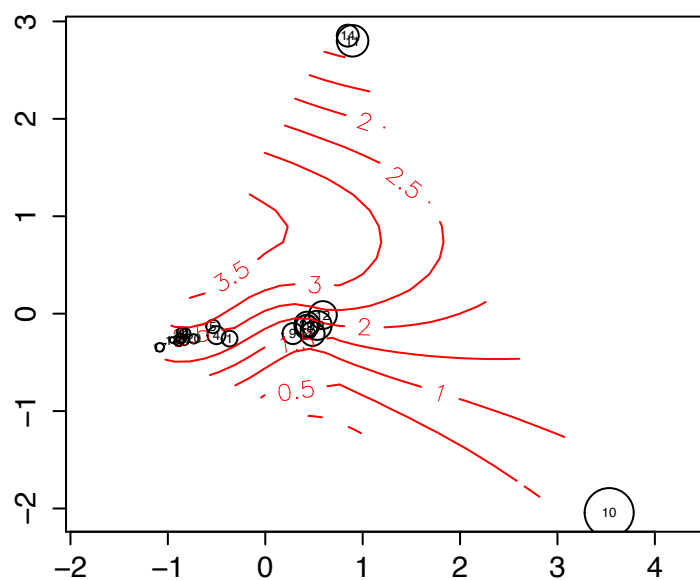
LX, June 2012 CO₂ ~ Sept 2012 Shannon



LX, June 2013 CO₂ ~ June 2013 Shannon

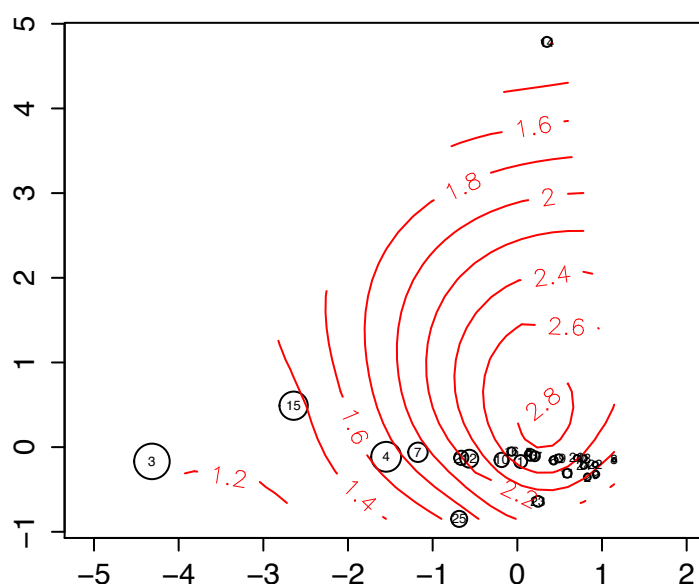


SN, June 2012 CO₂ ~ Sept 2012 Shannon

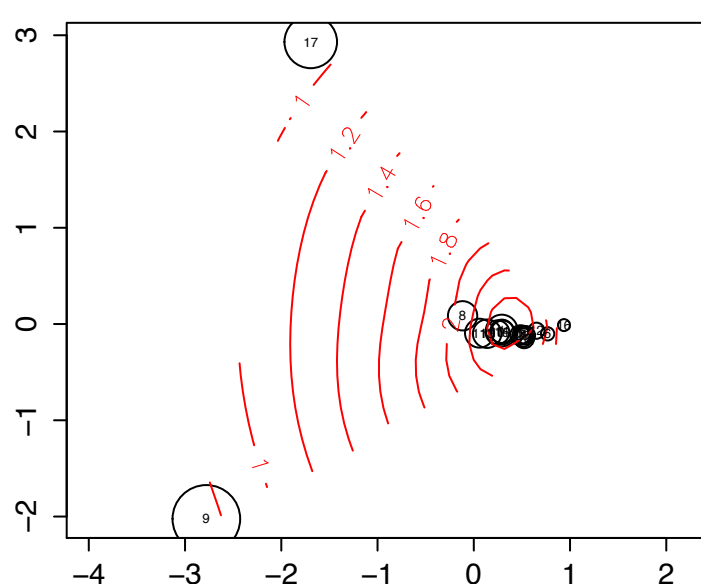
SN, June 2013 CO₂ ~ June 2013 Shannon

S4 B. *uclust* O-U-picking, non-farrelled

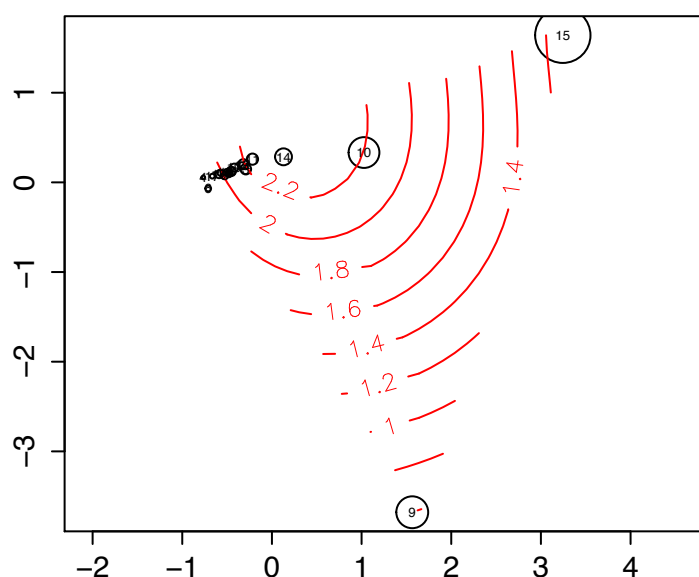
LC, June 2012 CO₂ ~ Sep 2012 Shannon



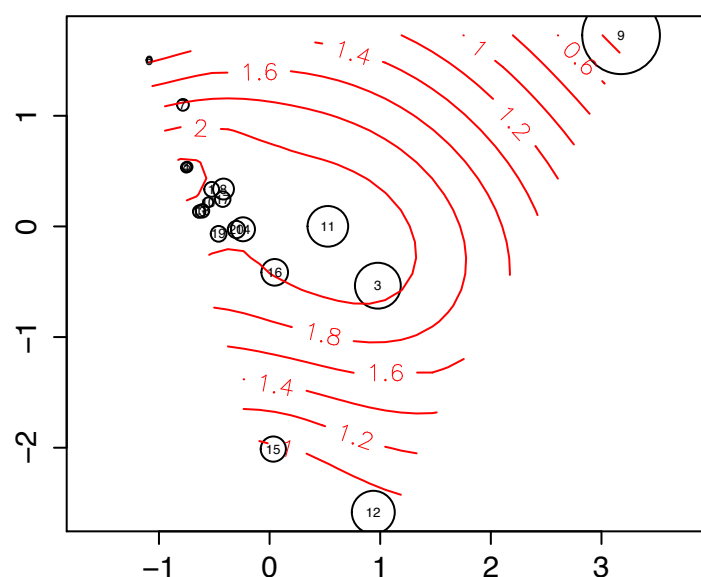
LC, June 2013 CO₂ ~ June 2013 Shannon



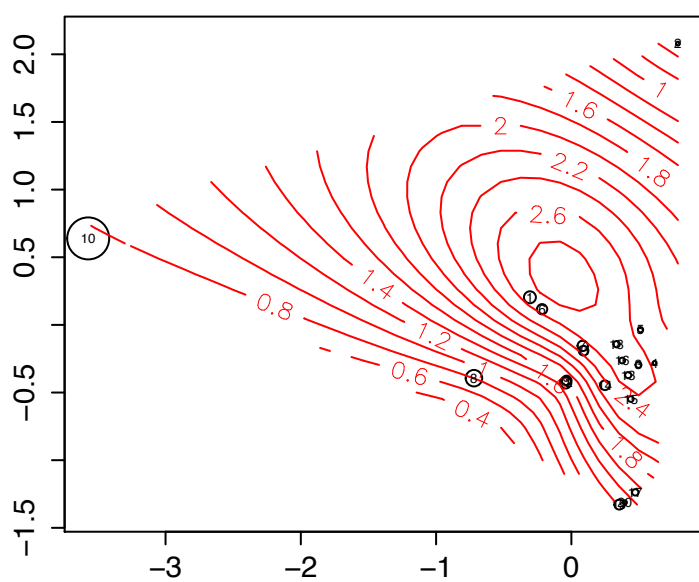
LX, June 2012 CO₂ ~ Sept 2012 Shannon



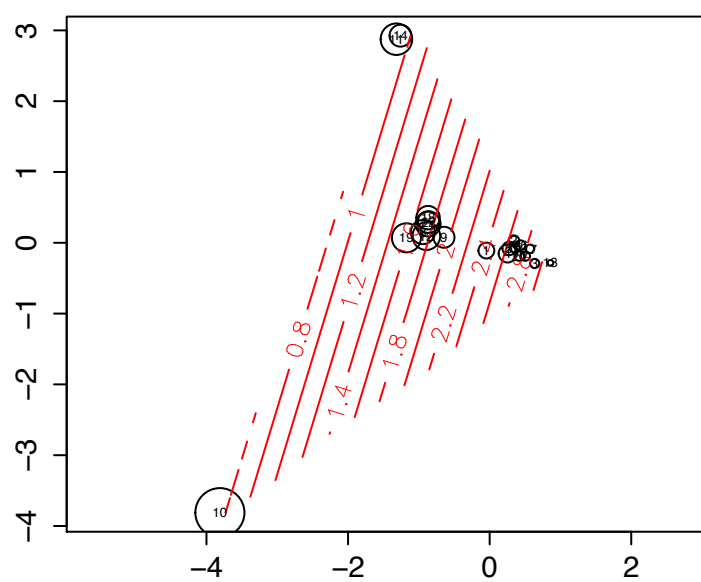
LX, June 2013 CO₂ ~ June 2013 Shannon



SN, June 2012 CO₂ ~ Sept 2012 Shannon

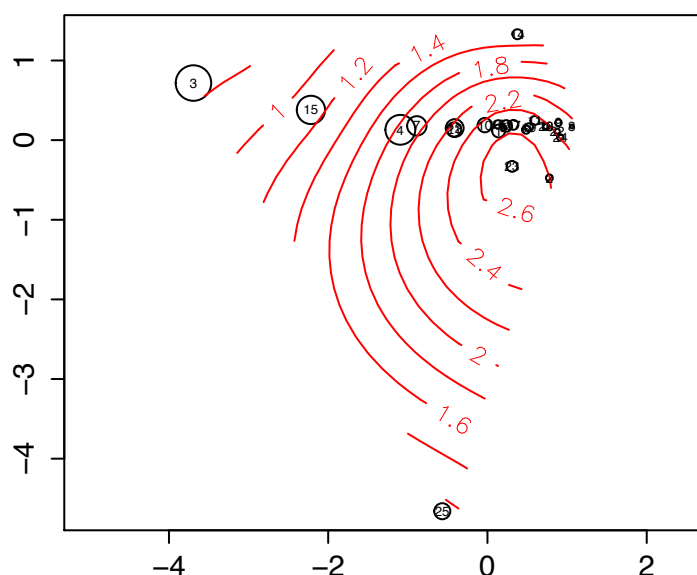


SN, June 2013 CO₂ ~ June 2013 Shannon

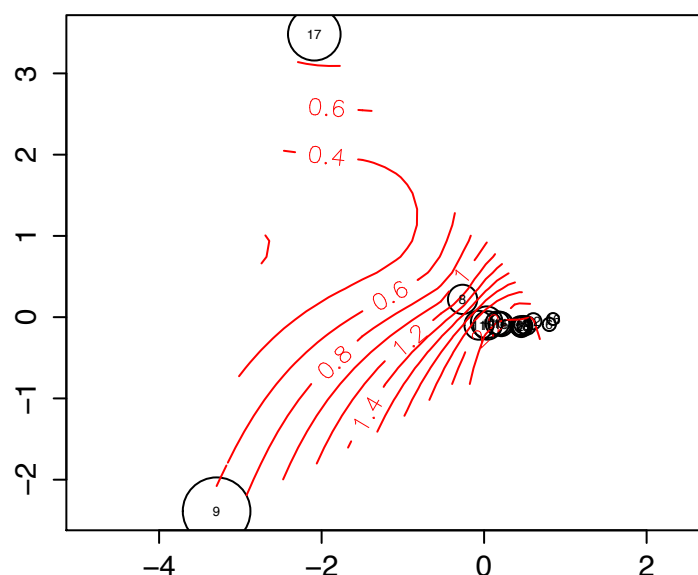


S4 C. *uclust* OTO-picking, rarefied

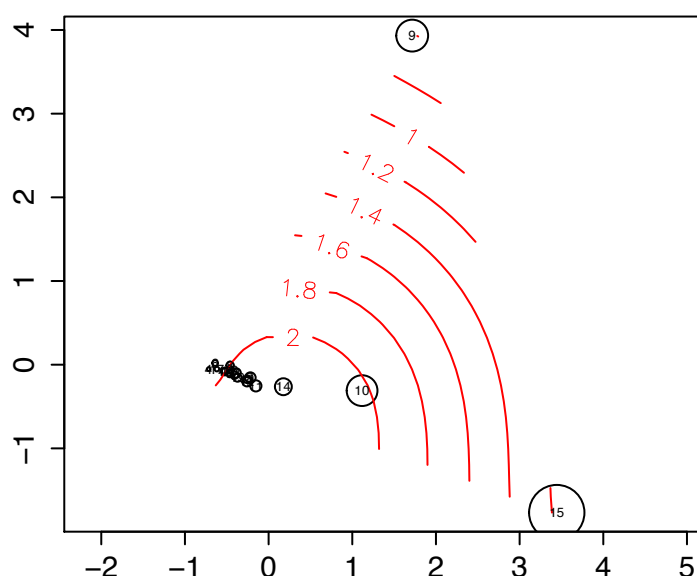
LC, June 2012 CO₂ ~ Sep 2012 Shannon



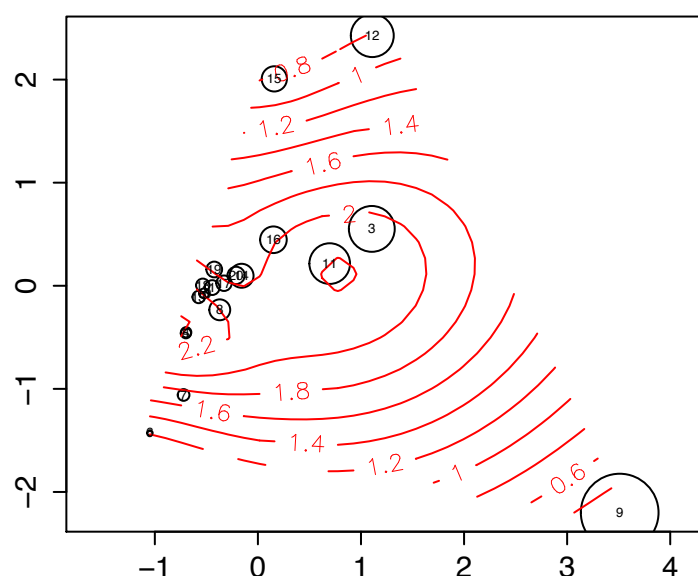
LC, June 2013 CO₂ ~ June 2013 Shannon



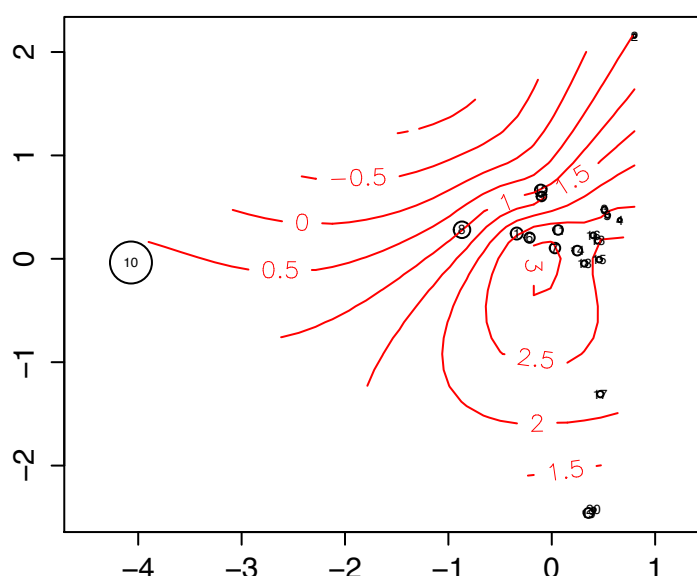
LX, June 2012 CO₂ ~ Sept 2012 Shannon



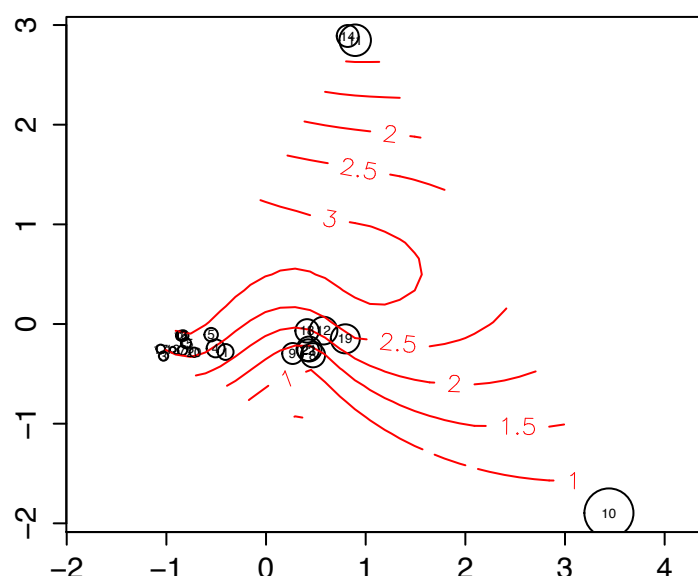
LX, June 2013 CO₂ ~ June 2013 Shannon



SN, June 2012 CO₂ ~ Sept 2012 Shannon



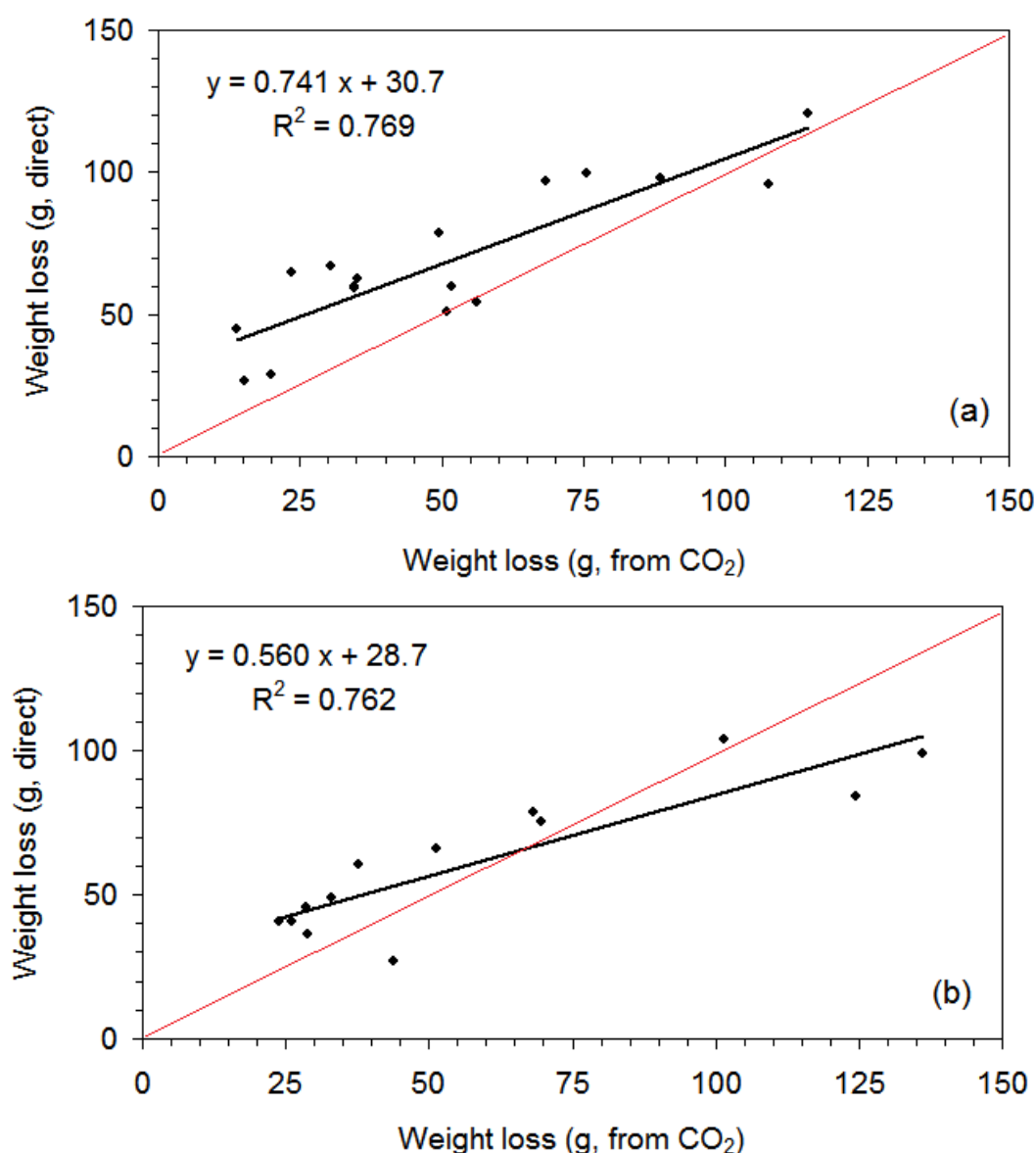
SN, June 2013 CO₂ ~ June 2013 Shannon

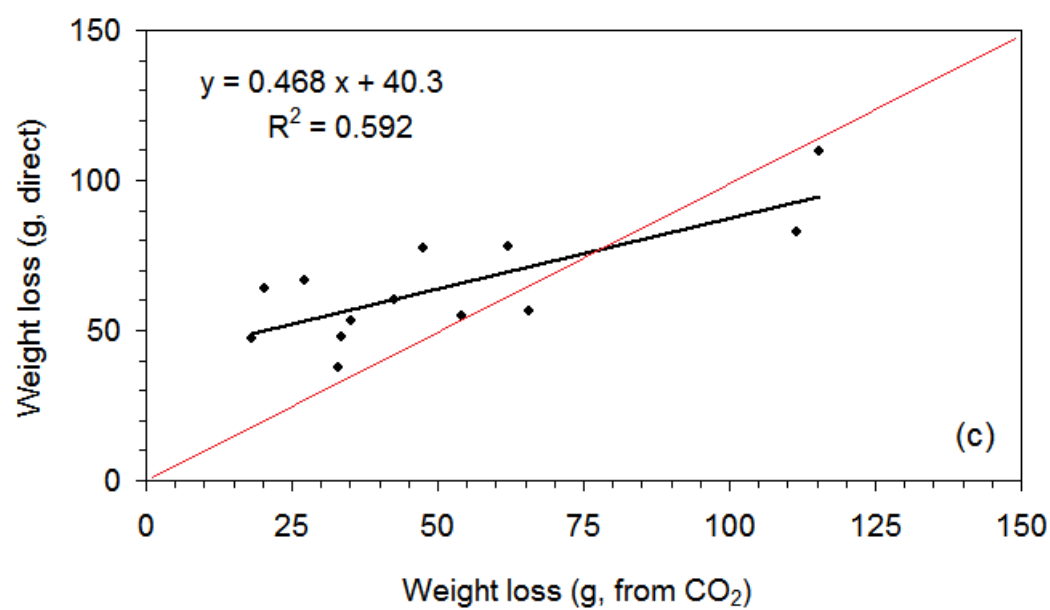


Higher fungal diversity is correlated with lower CO₂ emissions from dead wood in a natural forest:

S5 Gravimetric vs CO₂ estimated loss

Supporting Information S5. Mass loss from wood pieces (g over 3 years) as measured gravimetrically and as estimated from average CO₂ emission rates in decay class 1 (DKC1, top), decay class 2 (middle), and decay class 3 (bottom). Black lines are linear regressions and red lines represent 1:1 correspondences.





Higher fungal diversity is correlated with lower CO₂ emissions from dead wood in a natural forest:

SI Bioinformatic Command Scripts

```
# Background Information.
# 2012 samples (LC) were run in 3 regions in Jan 13, and 2 regions were
supplemented in Feb 13.
    2013 samples and 2012 samples (LX, SN) were run in 5 regions in Aug 13. 21
samples per region.
    On GSFLX454

##### split libraries
#####
#2012#
validate_mapping_file.py -m FungusMap_1.txt -o mapping_output
validate_mapping_file.py -m FungusMap_2.txt -o mapping_output
validate_mapping_file.py -m FungusMap_3.txt -o mapping_output
split_libraries.py -m FungusMap_1.txt -f 1.TCA.454Reads.fna -q
1.TCA.454Reads.qual -o split_library_output/1 -l 100 -L 500 -H 30 -z
truncate_only -b 10
split_libraries.py -m FungusMap_2.txt -f 2.TCA.454Reads.fna -q
2.TCA.454Reads.qual -o split_library_output/2 -l 100 -L 500 -H 30 -z
truncate_only -b 10 -n 42576
split_libraries.py -m FungusMap_3.txt -f 3.TCA.454Reads.fna -q
3.TCA.454Reads.qual -o split_library_output/3 -l 100 -L 500 -H 30 -z
truncate_only -b 10 -n 79479
split_libraries.py -m FungusMap_1.txt -f 7.TCA.454Reads.fna -q
7.TCA.454Reads.qual -o split_library_output/7 -l 100 -L 500 -H 30 -z
truncate_only -b 10 -n 143667
split_libraries.py -m FungusMap_2.txt -f 8.TCA.454Reads.fna -q
8.TCA.454Reads.qual -o split_library_output/8 -l 100 -L 500 -H 30 -z
truncate_only -b 10 -n 211778

#2013#
validate_mapping_file.py -m FungusMap_4.txt -o mapping_output
validate_mapping_file.py -m FungusMap_5.txt -o mapping_output
validate_mapping_file.py -m FungusMap_6.txt -o mapping_output
validate_mapping_file.py -m FungusMap_7.txt -o mapping_output
validate_mapping_file.py -m FungusMap_8.txt -o mapping_output
split_libraries.py -m FungusMap_4.txt -f 4.TCA.454Reads.fna -q
4.TCA.454Reads.qual -o split_library_output/4 -l 100 -L 500 -H 30 -z
truncate_only -b 10
split_libraries.py -m FungusMap_5.txt -f 5.TCA.454Reads.fna -q
5.TCA.454Reads.qual -o split_library_output/5 -l 100 -L 500 -H 30 -z
truncate_only -b 10 -n 86179
split_libraries.py -m FungusMap_6.txt -f 6.TCA.454Reads.fna -q
6.TCA.454Reads.qual -o split_library_output/6 -l 100 -L 500 -H 30 -z
truncate_only -b 10 -n 167521
split_libraries.py -m FungusMap_7.txt -f 7.TCA.454Reads.fna -q
7.TCA.454Reads.qual -o split_library_output/7 -l 100 -L 500 -H 30 -z
truncate_only -b 10 -n 256997
split_libraries.py -m FungusMap_8.txt -f 8.TCA.454Reads.fna -q
8.TCA.454Reads.qual -o split_library_output/8 -l 100 -L 500 -H 30 -z
truncate_only -b 10 -n 351216

#####Denoiser on QIIME pipeline
#####
#2012#
denoiser.py -i H2P9ZGK01.txt -f ../split_library_output/1/seqs.fna --primer
TCCTCCGCTTATTGATATGC -v -o denoise/1 -c -n 8
```

```
denoiser.py -i H2P9ZGK02.txt -f ../split_library_output/2/seqs.fna --primer
TCCTCCGCTTATTGATATGC -v -o denoise/2 -c -n 8
denoiser.py -i H2P9ZGK03.txt -f ../split_library_output/3/seqs.fna --primer
TCCTCCGCTTATTGATATGC -v -o denoise/3 -c -n 8
denoiser.py -i H3RH8HN07.txt -f ../split_library_output/7/seqs.fna --primer
TCCTCCGCTTATTGATATGC -v -o denoise/7 -c -n 8
denoiser.py -i H3RH8HN08.txt -f ../split_library_output/8/seqs.fna --primer
TCCTCCGCTTATTGATATGC -v -o denoise/8 -c -n 8
```

```
inflate_denoiser_output.py -c denoise/1/centroids.fasta -s
denoise/1/singletons.fasta -f ../split_library_output/1/seqs.fna -d
denoise/1/denoiser_mapping.txt -o inflated_1_seqs.fna
inflate_denoiser_output.py -c denoise/2/centroids.fasta -s
denoise/2/singletons.fasta -f ../split_library_output/2/seqs.fna -d
denoise/2/denoiser_mapping.txt -o inflated_2_seqs.fna
inflate_denoiser_output.py -c denoise/3/centroids.fasta -s
denoise/3/singletons.fasta -f ../split_library_output/3/seqs.fna -d
denoise/3/denoiser_mapping.txt -o inflated_3_seqs.fna
inflate_denoiser_output.py -c denoise/7/centroids.fasta -s
denoise/7/singletons.fasta -f ../split_library_output/7/seqs.fna -d
denoise/7/denoiser_mapping.txt -o inflated_7_seqs.fna
inflate_denoiser_output.py -c denoise/8/centroids.fasta -s
denoise/8/singletons.fasta -f ../split_library_output/8/seqs.fna -d
denoise/8/denoiser_mapping.txt -o inflated_8_seqs.fna
```

```
cat FungusMap_1.txt FungusMap_2.txt FungusMap_3.txt > Map_2012.txt
cat inflated_1_seqs.fna inflated_2_seqs.fna inflated_3_seqs.fna
inflated_7_seqs.fna inflated_8_seqs.fna > denoised_seqs_2012.fna
truncate_reverse_primer.py -f denoised_seqs_2012.fna -m Map_2012.txt -o
reverse_primer_removed_2012/
```

```
#2013#
denoiser.py -i IET0IJC04.txt -f split_library_output/4/seqs.fna --primer
TCCTCCGCTTATTGATATGC -v -o denoise/4 -c -n 8
denoiser.py -i IET0IJC05.txt -f split_library_output/5/seqs.fna --primer
TCCTCCGCTTATTGATATGC -v -o denoise/5 -c -n 8
denoiser.py -i IET0IJC06.txt -f split_library_output/6/seqs.fna --primer
TCCTCCGCTTATTGATATGC -v -o denoise/6 -c -n 8
denoiser.py -i IET0IJC07.txt -f split_library_output/7/seqs.fna --primer
TCCTCCGCTTATTGATATGC -v -o denoise/7 -c -n 8
denoiser.py -i IET0IJC08.txt -f split_library_output/8/seqs.fna --primer
TCCTCCGCTTATTGATATGC -v -o denoise/8 -c -n 8
```

```
inflate_denoiser_output.py -c denoise/4/centroids.fasta -s
denoise/4/singletons.fasta -f split_library_output/4/seqs.fna -d
denoise/4/denoiser_mapping.txt -o inflated_4_seqs.fna
inflate_denoiser_output.py -c denoise/5/centroids.fasta -s
denoise/5/singletons.fasta -f split_library_output/5/seqs.fna -d
denoise/5/denoiser_mapping.txt -o inflated_5_seqs.fna
inflate_denoiser_output.py -c denoise/6/centroids.fasta -s
denoise/6/singletons.fasta -f split_library_output/6/seqs.fna -d
denoise/6/denoiser_mapping.txt -o inflated_6_seqs.fna
inflate_denoiser_output.py -c denoise/7/centroids.fasta -s
denoise/7/singletons.fasta -f split_library_output/7/seqs.fna -d
denoise/7/denoiser_mapping.txt -o inflated_7_seqs.fna
inflate_denoiser_output.py -c denoise/8/centroids.fasta -s
denoise/8/singletons.fasta -f split_library_output/8/seqs.fna -d
denoise/8/denoiser_mapping.txt -o inflated_8_seqs.fna
```

```

cat FungusMap_4.txt FungusMap_5.txt FungusMap_6.txt FungusMap_7.txt
FungusMap_8.txt> Map_2013.txt
cat inflated_4_seqs.fna inflated_5_seqs.fna inflated_6_seqs.fna
inflated_7_seqs.fna inflated_8_seqs.fna > denoised_seqs_2013.fna
truncate_reverse_primer.py -f denoised_seqs_2013.fna -m Map_2013.txt -o
reverse_primer_removed_2013/

##### extract ITS2 region with ITSx
#####
#2012#
ITSx -i
reverse_primer_removed_2012/denoised_seqs_2012_rev_primer_truncated.fna -o
ITSx_output_2012
#use grep to remove all non fungal sequences from the file
ITSx_output_2012.ITS2.fasta
#restore the original QIIME headers to the ITSx output files
perl restore_headers.pl denoised_seqs_2012_rev_primer_truncated.fna
ITSx_output_2012/ITSx_output_2012_ITS2_F

#2013#
ITSx -i
reverse_primer_removed_2013/denoised_seqs_2013_rev_primer_truncated.fna -o
ITSx_output_2013
#use grep to remove all non fungal sequences from the file
ITSx_output_2013.ITS2.fasta
#restore the original QIIME headers to the ITSx output files
perl restore_headers.pl denoised_seqs_2013_rev_primer_truncated.fna
ITSx_output_2013/ITSx_output_2013_ITS2_F

#combine two years seqs#
cat ITSx_2012_output.ITS2_F.restored.fasta
ITSx_2013_output.ITS2_F.restored.fasta > ITSx_output_all_F.fasta

##### Denoise with USEARCH
#####
pick_otus.py -i ITSx_output_all_F.fasta -m usearch --word_length 64 -f
its_12_11_otus/rep_set/99_otus.fasta -g 1 -F intersection -o
ITSx_usearch_qf_intersection_0.99denoise -j 0.99

##### CROP OTU picking at 97% similarity with
crop/intel/1.33#####
CROP -i repr_set.fasta -o CROP.exact_otus -s -b 86 -z 882

#Downstream processing of CROP output, 2849 OTUs #
#Use TextWrangler to replace commas in CROP.exact_otus.cluster.list with tab
characters, creating CROP.exact_otus.cluster.tab.list
#Merge CROP and USEARCH pipeline OTU maps (see
http://qiime.sourceforge.net/scripts/merge_otu_maps.html for what this means).
merge_otu_maps.py -i
ITSx_usearch_qf_intersection_0.99denoise/ITSx_output_all_F_otus.txt,CROP.exact_o
tus.cluster.tab.list -o merged_otu_crop97_map.txt

# making OTU tables #
make_otu_table.py -i merged_otu_crop97_map.txt -o
merged_otu_table_crop97_notax.biom

#nonsingleread #

```

```

mkdir nonsingleread
filter_otus_from_otu_table.py -i merged_otu_table_crop97_notax.biom -o
nonsingleread/otu_table_crop97_notax_nonsingleread.biom -n 1

#Assign taxonomy by Claident#
clidentseq blastn -strand plus -task blastn -word_size 9 end --
bdb=fungi_ITS_genus --method=NNC+QC --numthreads=6 CROP.exact_otus.cluster.fasta
retri_nncqc_neighb_seq.txt
classigntax --taxdb=fungi_ITS_genus retri_nncqc_neighb_seq.txt
claident_nncqc_identresult.txt

#add taxonomy into otutable#
#perl file 'table_add_taxonomy_QIIME.pl' written by XXW and YCX
perl table_add_taxonomy_QIIME.pl -i1 otu_table_crop97_notax_nonsingleread.txt
-i2 claident_nncqc_identresult_edited.txt -o otutable_claident_nncqc_tax.txt

#add 'Unassigned' after otus failed to assign#

#convert txt file to biom
biom convert -i otutable_claident_nncqc_tax_edit2.txt -o
otutable_claident_nncqc_tax_edit2.biom --table-type="OTU table" --process-obs-
metadata taxonomy

biom convert -i otutable_crop_claident_final.txt -o
otutable_crop_claident_final.biom --table-type="OTU table" --process-obs-
metadata taxonomy

#taxonomy summary#
summarize_taxa_through_plots.py -i otutable_claident_nncqc_tax_edit2.biom -o
otu_taxa_summary2 -m map_2yearsall.txt

summarize_taxa_through_plots.py -i otutable_crop_claident_final.biom -o
otu_taxa_summary_final -m map_2yearsall.txt

##### UCLUST OTU picking at 97% similarity V1
#####
pick_open_reference_otus.py -i ITSx_output_all_F.fasta -r
its_12_11_otus/rep_set/97_otus.fasta -o ucrss_ITSx_all/ -p params_97.txt --
suppress_align_and_tree

#params_97.txt as followed#
assign_taxonomy:rdp_max_memory 20000
pick_otus:enable_rev_strand_match True
pick_otus:max_accepts 20
pick_otus:max_rejects 500
pick_otus:stepwords 20
pick_otus:word_length 12
assign_taxonomy:id_to_taxonomy_fp
its_12_11_otus/taxonomy/97_otu_taxonomy.txt
assign_taxonomy:reference_seqs_fp its_12_11_otus/rep_set/97_otus.fasta
beta_diversity:metrics bray_curtis

# making OTU tables #
#nonsingleread #
mkdir nonsingleread
filter_otus_from_otu_table.py -i otu_table_mc2_w_tax.biom -o
nonsingleread/otu_table_mc2_w_tax_nonsingleread.biom -n 1

```

```
# convert biom to txt (qiime 1.8)#
biom convert -i otu_table_mc2_w_tax_nonsingleread.biom -o
otu_table_mc2_w_tax_nonsingleread_tax.txt -b --header-key taxonomy

#delete 1: the samples are not sequences in batch, 2: delete OTUs counts
sum=0/1
#convert back to biom
biom convert -i otutable_uclust_tax_final.txt -o
otutable_uclust_tax_final.txt.biom --table-type="OTU table" --process-obs-
metadata taxonomy

#taxonomy summary#
summarize_taxa_through_plots.py -i otutable_uclust_tax_final.txt.biom -o
otu_taxa_summary2 -m map_2yearsall.txt
```